

Copyright is owned by the Author of the thesis. Permission is given for a copy to be downloaded by an individual for the purpose of research and private study only. The thesis may not be reproduced elsewhere without the permission of the Author.

FINITE SIZE EFFECTS IN THE STUDY OF EQUATION OF STATE
FOR THE NUCLEI WITH SKYRME FORCE

A THESIS PRESENTED IN PARTIAL FULFILMENT OF
REQUIREMENTS FOR THE DEGREE OF MASTER
IN
PHYSICS

At MASSEY UNIVERSITY, PALMERSTON NORTH
NEW ZEALAND

KHLOOD FAHAD AL HARTHI

2017

ABSTRACT

The equation of state for symmetric nuclear matter and finite nuclei has been investigated using self-consistent Hartree Fock approach. Several versions of Skyrme effective interaction and Hill-Wheeler formula are employed in the calculation. The finite size effect parameter a_F , which is introduced into the Hill-Wheeler formula, is determined by comparing theoretical calculations and experimental results for the zero temperature properties. The dependence of a_F on the effective interaction employed has been studied. It was found that different versions of Skyrme force lead to different values for a_F apart from SKI and SKIII which gave a similar value. Also, the a_F values obtained with Skyrme interaction were different from what was obtained with Gogny force with the exception of SKV interaction which gave a value of $a_F = 0.35$ identical to the value obtained with D1 Gogny interaction. The critical points of the first order phase transition for the nuclear matter and finite size nuclei calculated with the several versions of Skyrme force were different from each other. The largest value of critical temperature for nuclear matter is given by SKV force as $T_c = 39.45$ MeV, while SKIII interaction gives the smallest value as $T_c = 21.65$ MeV. Similarly, the largest value of the critical density is given by SKV interaction. The critical points depend on the number of nucleons in the system and T_c decreases as the number of nucleons in the system decreases.

ACKNOWLEDGEMENT

First and foremost I thank my God, Allah, who has given me the power to believe in my passion and skills to accomplish this work.

I would like to acknowledge the support and training I have received during my thesis research from my supervisor Dr.Fu-Guang Cao whose expertise and guidance have been invaluable. Special thanks for his encouragement and patience.

I would like to express my sincere thanks to my co-supervisor Prof.Tony Signal for his support during my research. I would like to thank Dr.Khaled Hassaneen for significant discussions about my research. Special thanks to Dr.Eka Wijaya and Ahowd Alfahad, who as good friends, were always willing to help and give their best suggestions.

My deepest appreciation goes to my husband, Saeed Alharthi, for all of the sacrifices he has made, which made the undertaking of this thesis possible and special thanks for his help and great patience. My appreciation is extended to my children who missed spending time with their mother during the researching course. I have been extremely lucky to have a lovely daughter, Rasil, who has been always taking care of her siblings and cheering me up. Thank you, Rasil, for your great help.

Lastly, I acknowledge the financial assistance provided by the Saudi Arabia government. Without this support I could not have undertaken this research. Also, I would like to thank the staff at Massey University who have assisted me whenever needed.

This thesis is specially dedicated to my parents, sisters and brothers, whose encouragement and support have been really significant in my pursuing a successful academic career.

TABLE of CONTENTS

1	Introduction	1
2	Nuclear Many-Body System	4
2.1	Nuclear Matter	4
2.2	Nuclear Force	5
2.3	Nuclear Matter Phases	6
3	Mean Field Theory	9
3.1	Hartree Fock Formalism	10
3.2	Skyrme Effective Interaction	14
3.3	Gogny Effective Interaction	15
3.4	Skyrme Hartree Fock Quations	16
3.4.1	The Zero-Range Term	17
3.4.2	The Density Dependence Term	18
3.4.3	The Momentum Dependence Term	19
3.4.4	The Spin-Orbit Term	23
4	The Equation of State Calculation	27
4.1	The Model Description	27

4.1.1	Symmetric Nuclear Matter	28
4.1.2	Finite System	29
4.2	Zero Temperature Properties	31
4.3	Liquid-Gas Phase Transition	34
4.4	Critical Temperature	35
4.5	Chemical Potential	35
5	Results and Discussion	37
5.1	Zero Temperature Properties	37
5.1.1	Infinite Nuclear Matter	37
5.1.2	Finite Size Effect Parameter and Saturation Properties	39
5.2	Liquid-Gas Phase Transition	42
5.2.1	Infinite Nuclear Matter	42
5.2.2	Finite Size Systems	45
6	Summary and Conclusion	49
A	Appendix	54

List of Figures

1	The hierarchy of the nuclear matter structure. Nuclei consist of nucleons (i.e. protons and neutrons) and nucleons consist of quarks	5
2	The collision of two fragments in nuclear matter.	7
3	The temperature of the fragments in a collision of two nuclei (^{197}Au) as a function of the excitation of energy per nucleon. The behaviour of the temperature can be understood as a phase transition in nuclear matter.	8
4	The explanation of the mean field method where particles interact through a self-bound mean field instead of many-body interaction in the initial problem	9
5	The steps to solve Hartree Fock equations self-consistently. Firstly, the single particle states have to be selected. Then, one can compute the mean field Hamiltonian. New states of the single particle are found by diagonalizing the Hamiltonian. This procedure is repeated until the convergence is realized.	13
6	The indication of the fermi level distribution, where the energy, ε_i , and the occupation number, n_i , for the single particles are lower than the fermi energy, ε_f	34
7	The energy \sim density isotherms for nuclear matter given by the five sets of Skyrme interaction.	38
8	The energy \sim density isotherms for $^{56}_{28}\text{Ni}$ obtained from Eq.(5.2) with $a_F = 1.0$ and 0.55 given by SKIV interaction.	42
9	The chemical potential \sim density isotherms for nuclear matter given by SKI interaction at different temperatures.	44
10	The chemical potential \sim density isotherms for nuclear matter given by the five sets of Skyrme interaction at $T=16$ MeV.	44

11	The chemical potential \sim density isotherms in different sizes given by SKIV interaction at $T=16.0$ MeV.	47
12	The chemical potential \sim density isotherms for $N=1000$ at different temperatures given with SKII interaction.	47
13	The chemical potential \sim density isotherms in different sizes ($N=100, 1000, 10000$) given with Eq.(4.4) and SKV interaction at $T=16.0$ MeV.	48
14	The chemical potential \sim density isotherms in different sizes ($N=100, 1000, 10000$) given with Eq.(5.2) and SKV interaction at $T=16.0$ MeV.	48

List of Tables

1	The parameters for different versions of Skyrme interaction. The values are taken from Ref.[24].	14
2	The parameters of Gogny D1 effective interaction. The values are taken from Ref.[2].	15
3	The ground state energies for six typical nuclei employing Eq.(4.4) and Gogny interaction found in Ref.[2].	30
4	The saturation properties of nuclear matter calculated with different versions of Skyrme interaction.	38
5	The calculated values of a_F with different versions of Skyrme interaction. . .	40
6	The saturation properties for different nuclei obtained with different versions of Skyrme interaction, where (Exp.) means the experimental data.	41
7	The values of some properties for nuclear matter obtained in Ref.[24] employing several sets of Skyrme interaction, where the effective masses at the critical density and at the saturation density are denoted by $(m^*/m)_c$ and $(m^*/m)_o$, respectively.	41
8	The critical values of the temperature $T_c(MeV)$ and the density $\rho_c(fm^{-3})$ calculated in this work and in Ref.[24] for an infinite nuclear matter with different versions of Skyrme interaction.	43
9	The critical values of the temperature $T_c(MeV)$ and the density $\rho_c(fm^{-3})$ for different sizes calculated with different versions of Skyrme interaction.	46
10	The values of the critical points for different sizes (N=100, 1000, 10000) obtained in a previous study [15] with Eq.(4.4) using Skyrme interaction. . .	46

1 Introduction

The investigation of properties of nuclear matter (NM) and finite nuclei is one of the significant subjects in nuclear physics and astrophysics and has been receiving great attention. The main motivation behind numerous theoretical studies is the developments of heavy-ion collisions [1, 2]. Empirically, heavy-ion collisions have been done [3] as cited in [4], to obtain unknown properties of hot nucleus described in collisions [5, 6]. Theoretically, a number of works have been devoted to the study of the equation of state (EOS) of nuclear matter and the critical features [7–15], by using several methods of calculations and various effective nucleon-nucleon (NN) interactions [16].

The heavy-ion experiments show evidence for a transition from the liquid to a gas phase where the average distance of the interparticle is larger than the interaction range of the interparticle [17]. In the line with a phase transition is a critical temperature above which the gaseous phase can exist [18]. In view of empirical results of relativistic heavy-ion collisions, the critical temperature is a very interesting point [19]. In an earlier paper published by Jaqamin, Mekjian and Zamick [18], this point was demonstrated in a system of infinite NM where the calculations were carried out without considering the coulomb effects.

In Ref. [20], it was predicted that the number of nucleons produced in any nuclear collision cannot extend more than a few hundred nucleons. Therefore, the properties of an infinite system are not adequate in describing a finite system. It is worth pointing out that the boundaries of nucleus might play a great role in performing the calculations. The finite size effect cannot be ignored in the calculations of the equation of state and critical phenomena, due to the fact of its large effect [18].

Jaqamin and his co-workers [20] have demonstrated that such a finite size effect can be taken into account by including the formula of Hill and Wheeler in the calculations. However, the validity of the EOS of thermodynamic properties in a finite size system is not assured. In other words, the geometry of interfacial region in finite nuclear matter can affect the measuring of some quantities such as pressure [18]. As it is hazardous to determine the

pressure in a finite system, they have taken advantage of similar results that have been found between the EOS produced by $(P - \rho)$ isotherms and those given by $(\mu - \rho)$ isotherms in the case of infinite NM [18].

Therefore, a successful attempt has been done [20], to investigate the liquid-gas phase transition in a system consisting of a limited number of nucleons where the finite size effect and coulomb interaction are included. They have suggested a procedure for the study of the critical points in a finite size system by investigating the relation between the chemical potential and the density $(\mu - \rho)$ isotherms instead of the pressure and the density $(P - \rho)$ isotherms. It was found that the finite size effect and coulomb interaction could reduce the critical temperature by about $5 \sim 10$ MeV and about $1 \sim 3$ MeV, respectively [20].

Furthermore, they demonstrated that studying the EOS of a finite system by working with chemical potential $\mu = \mu(\rho)$ instead of working with pressure $P = P(\rho)$ would be a promising method since it is easier to calculate the chemical potential than the pressure. It was pointed out [21] that the rearrangement effect needs to be included in the Hartree Fock approximation with density dependent versions of effective NN interaction. At finite temperature, Su and Lin showed [22] that the rearrangement effect can be taken into account by a rearrangement term in the chemical potential.

Wang and Yang [23] as cited in [2] pointed out that adopting directly the formula of Hill-Wheeler in the EOS calculations for nucleus as in Refs.[16, 20] cannot correctly predict binding energies and other zero temperature properties. Cao and Yang [2] modified the Hill-Wheeler expression in the study with Gogny effective interaction in the framework of Hartree Fock approximation aiming to produce better agreement between theoretical calculations and experimental results for the nucleus properties at zero temperature. Such an adjustment can be done by introducing a finite size effect parameter (a_F) in the formula of Hill-Wheeler. The value obtained for a_F in [2] is $a_F = 0.35$. It is interesting to study whether the value of a_F depends on the effective interaction employed.

In the present work, we aim to study the zero temperature properties and liquid-gas phase transition for the NM and finite nuclei by employing Skyrme effective interaction and the Hill-Wheeler formula. Our approach is based on Hartree Fock approximation in which the mean field is constructed from the effective interaction between particles in a self-bound manner. This method has a great advantage over the other methods in the NM calculations due to its ability to simplify a many-body problem to one-body problem.

The selection of effective NN interaction plays an essential role in studying the gross properties of NM and phase transition [24]. There are several types of the effective interactions, and each type is normally introduced into different parameter sets. Among these effective interactions the most popular choices are Gogny interaction and Skyrme interaction. The latter will be employed in our study. The versions that will be used in this study are SKI, SKII, SKIII, SKIV, and SKV interactions.

This thesis is organized according to the following outline. A brief review of many-body theory is given in Chapter 2. The mean field theory and the effective interaction are presented in Chapter 3. This chapter is mostly devoted to reviewing in detail Hartree Fock mean field method and Skyrme effective interaction. The formulisms used in the EOS calculation are derived in Chapter 4. We determined the finite size parameter a_F by comparing theoretical calculations and experimental data for the binding energies for a set of nuclei, and then we computed the critical temperature for the first order phase transition. Su and Lin [15, 24] have calculated the critical temperature for the liquid-gas phase transition of NM system using a real time Green's function method and Skyrme interactions. Our findings will be presented and compared with their results in Chapter 5. Also the value for the finite size effect parameter that has been found in [2] using Gogny interaction will be compared with that found here employing Skyrme interaction. Finally, summary and conclusion are given in Chapter 6.

2 Nuclear Many-Body System

The quantum many-body theory has played an essential role in describing the properties of a system containing a large number of particles. Generally, this theory provides sufficient tools to describe several systems, starting from the inner structure of the nucleon to the enormous objects in outer space. A big picture of many-body systems is that we can generalize a large number of varied problems in a common approximation. This picture makes the many particles theory take a significant place in the physics area. Although the initial discovery of this theory was in the fifties, it is still an important source of theoretical studies for physicists [25]. In fact, it requires a deep understanding of different mathematical approximations such as Hartree Fock approach, in order to treat the many-body problem [26].

In the standard nuclear physics, the many-body problem has a simple definition. At the first step, one selects the particles which are the nucleons, i.e. the neutron and the proton. Then, the interaction between the chosen particles is given. After that the Schrödinger equation should be solved initially. To make the problem simpler, one usually considers an infinite system of nucleons with same number of protons and neutrons. This homogeneous system corresponds to symmetric nuclear matter, and the coulomb interactions among protons are often neglected. It means that one can treat nuclear matter as a large nucleus to depict qualitatively the interior of the neutron stars and heavy nuclei [27].

2.1 Nuclear Matter

Nuclear matter is composed of a huge number of nucleons which are composed of even smaller objects known as quarks. The hierarchy of the nuclear matter constitutions is depicted in Fig.1. Moreover, NM is considered as an idealized system of elementary particles interacting via strong interactions, i.e. nuclear force. Since the protons are charged particles, the coulomb interaction should be accounted in addition to the nuclear force [28]. Generally speaking, as these subatomic particles are described by the statistics of Fermi-Dirac, they

are characterized as fermions. According to that their wave functions, $\Phi \equiv \Phi(r, s, \tau)$, can be propagated into a momentum space with spin ($s = \uparrow, \downarrow$) and isospin $\tau = p, n$ [29].

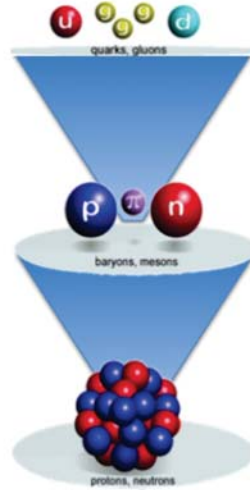


Figure 1: The hierarchy of the nuclear matter structure. Nuclei consist of nucleons (i.e. protons and neutrons) and nucleons consist of quarks (Lacroix, 2011, P.10).

2.2 Nuclear Force

One of the essential aims of theoretical physics in NM is to determine the bulk nuclear properties by using a nucleon-nucleon force. However, the information of nuclear forces is not yet completed due to the complexity associated with systems involving a large number of nucleons [29]. There are three methods for deriving nuclear force. The first one is that the interaction between nucleons is derived by the exchange of meson and this force was predicted by Yukawa. In this case, the interaction between nucleons is called a realistic force. The second one is a phenomenological method in which the nucleus is treated as a system consisting of N -nucleons that interact among themselves where the most fundamental interaction mainly happens between two-nucleons. This force is called a phenomenological effective interaction. The third way depends on the theory of effective field to construct the

force between nucleons, and thereby the other particles which ignored in other methods are included [30].

2.3 Nuclear Matter Phases

Liquid-gas phase transition has been observed in the experiments of heavy-ion collisions. It means that there are two distinct phases coexistence in NM at certain temperature range [31]. Fig.2 indicates a collision of two large fragments in nuclear matter. As we can see, the friction between the two major fragments leads them to heat up. Then, individual nucleons and smaller fragments are produced in this reaction. In such reactions, the fragments temperature and the energy provided to the system can be measured.

We can determine the temperature from the Maxwell distribution and calculate the total energy from detecting all the nucleons generated in the final state. As a matter of fact, the contribution of the energy supplied to the particles is separated from the lost energy during the collision. The temperature of the fragments depends on the energy added to the system.

In Fig.3 one can observe that the temperature increases rapidly as the excitation energies (E/N) are increased up to about 4 MeV/Nucleon. In the region between 4 MeV and 10 MeV, it is found that the temperature remains steady, while at higher energies it grows strongly. This behaviour is similar to that found in the water evaporation process where the phase transition from liquid into vapor is observed around the boiling temperature. In nuclear matter case, although the energy is supplied to the system, the temperature does not change until the system undergoes a phase transition [32].

Therefore, we can describe the temperature dependence explained above as a liquid-gas phase transition of nuclear matter. The logical interpretation for the phase transition is that nucleons form a layer around the nucleus in a gaseous phase when the temperature is at 4 MeV. This layer of nucleons does not steam, but it exchanges energy with the liquid nucleus to be in equilibrium. The heating up of the nucleon gas can only happen if the nucleon liquid evaporates completely.

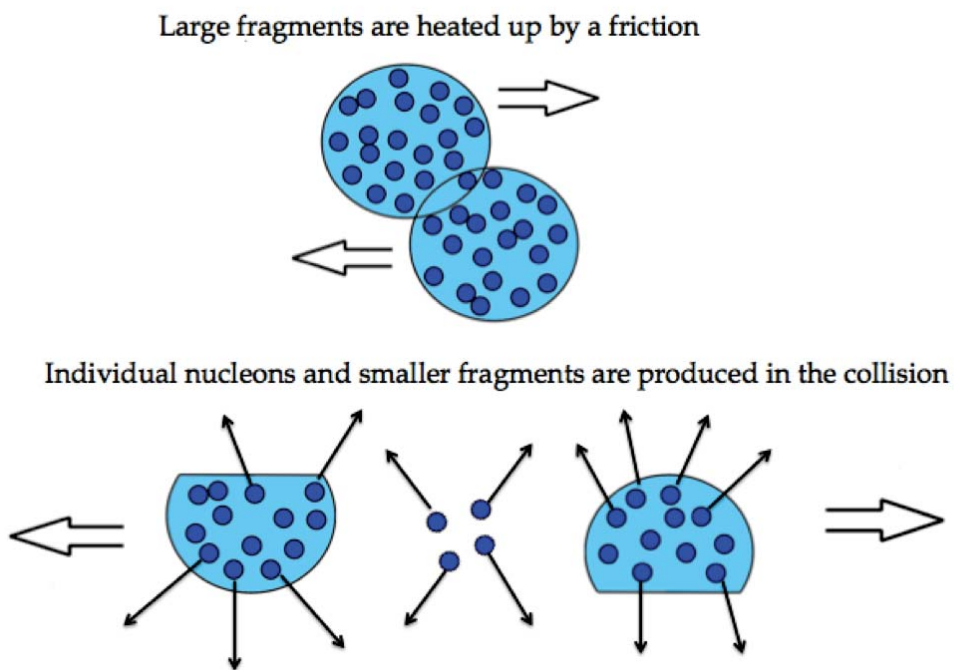


Figure 2: The collision of two fragments in nuclear matter (Povh et al., 1995, P.317).

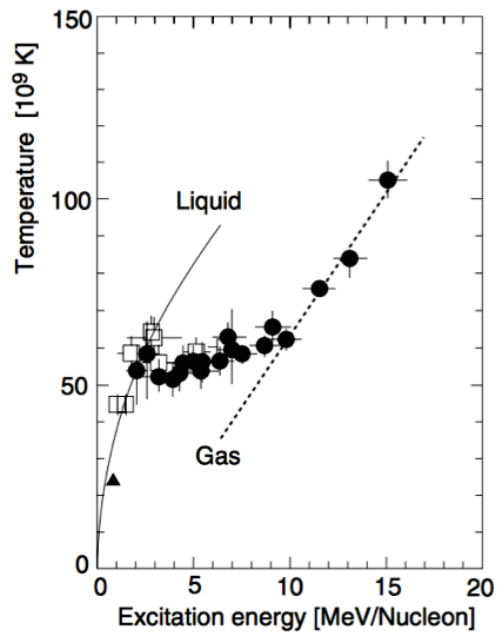


Figure 3: The temperature of the fragments in a collision of two nuclei (^{197}Au) as a function of the excitation of energy per nucleon. The behaviour of the temperature can be understood as a phase transition in nuclear matter (Povh et al., 1995, P.318).

3 Mean Field Theory

The self-consistent mean field approach has played a central part in providing a great understanding of microscopic quantum mechanical matter. It is a fundamental technique in the study of a many-body system where the exact solution of the problem is unknown [28]. In this technique, the many-body problem is systematically mapped onto a one-body density matrix. The philosophy of the mean field scheme is illustrated in Fig.4.

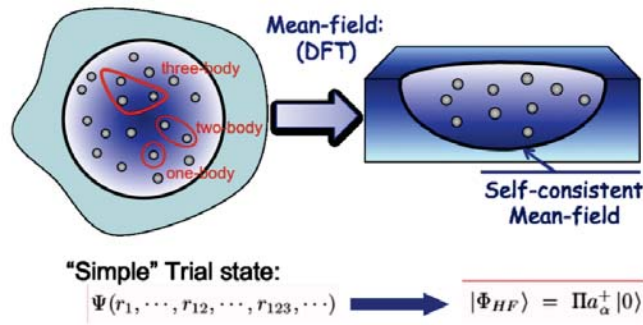


Figure 4: The explanation of the mean field method where particles interact through a self-bound mean field instead of many-body interaction in the initial problem (Lacroix, 2011, P.10).

One of the main procedures to introduce the mean field is based on choosing a set of single particle wave functions that are used to build a density matrix of one-body. Therefore, the Hamiltonian of observing system can be formed as the density functionals. As reported by Hohenberg-Kohn Theorem [33], generally, the information of these densities may be used to infer a clear description about the wave functions of this system and also the ground state observables. This is convenient since the one-body density matrix includes the same information of the ground state system of N single particle wave functions. As a consequence, the ground state energy is the most significant observable which can be obtained by minimizing the energy with respect to the density of the single particle, and this can be achieved by the variational principle. In fact, an explicit description for the NM and nuclei properties can be obtained successfully by applying the mean field theory within a system based on Hartree Fock approximation [34].

3.1 Hartree Fock Formalism

The main concept of the Hartree Fock approach is that the mutual interactions between particles can cause an average potential which can be felt by each interacting nucleon. Basically, the nucleus is considered as a system of many fermions which means any state of nucleus must be related to an antisymmetric wave function under the exchange of any two nucleons [29].

In the Hartree Fock (HF) approximation the wave function Φ of ground state for any nucleus with N nucleons is a Slater determinant which is constructed from a complete orthonormal set of the single particle wave functions [35]. Such states are known as the HF basis, $\varphi_i(r_i, s_i, \tau_i)$ where r_i, s_i, τ_i denote the coordinates of space, spin and isospin of the i -th nucleon, respectively. The form of the Slater determinant can be written as:

$$\Phi_{HF}(r, s, \tau) = \frac{1}{\sqrt{N!}} \begin{vmatrix} \varphi_1(r_1, s_1, \tau_1) & \varphi_2(r_1, s_1, \tau_1) & \dots & \varphi_N(r_1, s_1, \tau_1) \\ \varphi_1(r_2, s_2, \tau_2) & \varphi_2(r_2, s_2, \tau_2) & \dots & \varphi_N(r_2, s_2, \tau_2) \\ \vdots & \vdots & \ddots & \vdots \\ \varphi_1(r_N, s_N, \tau_N) & \varphi_2(r_N, s_N, \tau_N) & \dots & \varphi_N(r_N, s_N, \tau_N) \end{vmatrix}$$

Initially, in any particular calculations, the exact picture for the single particle states is undetermined. However, it is possible to approximate it by oscillator wave functions [36], where the number of the single particle states represents the number of nucleons in the nucleus.

It is worth starting with the full many-body Hamiltonian for a system consisting of N -particles that can be written in terms of a sum of kinetic energies and two-body potentials [37],

$$H = \frac{\hbar^2}{2} \sum_i^N \frac{\vec{\nabla}_i^2}{m_{\tau_i}} + \frac{1}{2} \sum_{i \neq j}^N V(r_i, r_j), \quad (3.2)$$

where $V(r_i, r_j)$ is the interaction between two bodies which includes the effective NN interaction V_{ij}^{NN} as well as the coulomb interaction V_c^{NN} .

From the expectation value of the Hamiltonian with respect to the HF wave function Φ_{HF} , the total energy (E) of the ground state can be found by

$$\begin{aligned}
E_{HF}^o &= \langle \Phi_{HF} | H | \Phi_{HF} \rangle \\
&= \sum_{i=1}^N \langle i | t | i \rangle + \frac{1}{2} \sum_{i,j=1}^N \langle ij | V | ij \rangle - \frac{1}{2} \sum_{i,j=1}^N \langle ij | V | ji \rangle \\
&= \sum_{i=1}^N \int dr \varphi_i^*(r) \left(-\frac{\hbar^2}{2m} \nabla_i^2 \right) \varphi_i(r) \\
&\quad + \frac{1}{2} \sum_{i,j=1}^N \int \int dr dr' \varphi_i^*(r) \varphi_j^*(r') V(r, r') \varphi_i(r) \varphi_j(r') \\
&\quad - \frac{1}{2} \sum_{i,j=1}^N \int \int dr dr' \varphi_i^*(r) \varphi_j^*(r') V(r, r') \varphi_i(r') \varphi_j(r).
\end{aligned} \tag{3.3}$$

The last term in Eq.(3.3) includes asymmetric states resulting from the exchange of any two nucleons in the system.

In order to derive HF equations, the expectation value of E has to be minimized to produce the lowest energy for the system, and this could be realized by applying a variational principle,

$$\frac{\delta}{\delta \varphi_i^*(r)} \left[E_{HF}^o - \sum_i^N \varepsilon_i \int dr \varphi_i^*(r) \varphi_i(r) \right] = 0, \tag{3.4}$$

where ε_i are the Lagrange multipliers, and we have

$$\frac{\delta \varphi_i^*(r')}{\delta \varphi_b^*(r)} = \delta_{ib} \delta(r - r').$$

It is useful to mention that the first derivative of the total E expectation value with respect to the overall wave function of the single particle has to be zero, and in order to achieve the normalization of the wave functions, the ε_i parameter has been added in Eq.(3.4).

Then, one can obtain the HF equations for the wave functions of the single particle,

$$\begin{aligned} & \left[-\frac{\hbar^2}{2m}\nabla^2 + \sum_i^N \int dr' \varphi_i^*(r')V(r, r')\varphi_i(r') \right] \varphi_b(r) \\ & - \sum_i^N \int dr' \varphi_i^*(r)V(r, r')\varphi_i(r')\varphi_b(r') = \varepsilon_b\varphi_b(r), \end{aligned} \quad (3.5)$$

where ε_i turn out to be the energies of a single particle. The second term in Eq.(3.5) is a local term which known as the direct or Hartree potential,

$$U_D(r) = \sum_i^N \int dr' \varphi_i^*(r')V(r, r')\varphi_i(r').$$

The last term in Eq.(3.5) is a non-local term and known as the exchange or Fock potential.

$$U_{ex} = \sum_i^N \varphi_i^*(r)V(r, r')\varphi_i(r').$$

Eq.(3.5) can be expressed as

$$-\frac{\hbar^2}{2m}\nabla^2\varphi_b(r) + U_D(r)\varphi_b(r) - \int dr' U_{ex}(r, r')\varphi_b(r') = \varepsilon_b\varphi_b(r). \quad (3.6)$$

This equation is similar to Shrödinger equation of one-body, apart from the non-local term, and its solution will be a set of single particle states. That means, however, there will be a close set of non-linear equations that require to be solved self-consistently by using the iteration method for a given effective force $V(r_1, r_2)$, as illustrated in Fig.5. Starting with an initial set for the wave functions $\varphi_i(r)$ of the single particle, one can solve the HF equation after calculating the direct term and the exchange term to obtain the new values of the wave functions $\varphi_i(r)$ and energies (ε_i) for the single particle. This process is repeated until the desire accuracy is achieved [28].

Within the mean field method, the investigated system may be determined by selecting the relevant potential of the two-body. For all interacting nucleons in the system, the Coulomb and kinetic interactions are independent of $V(r_1, r_2)$ which need well-founded approximation to drive them [38], and the potential $V(r)$ can be calculated in various ways [34].

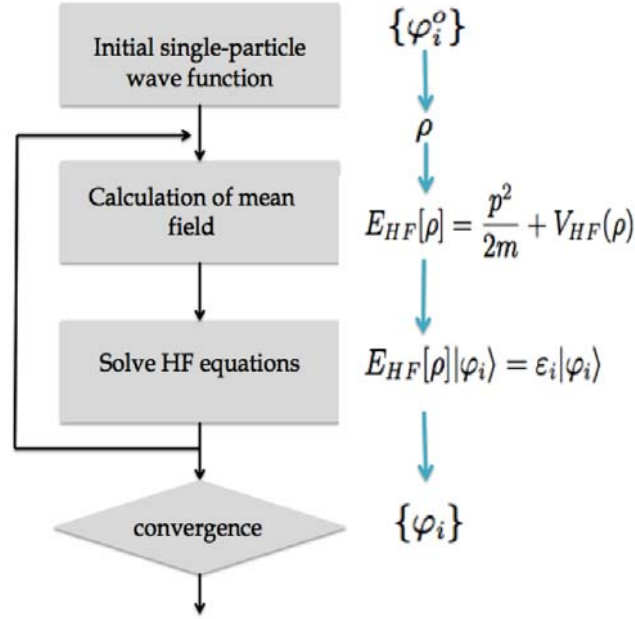


Figure 5: Steps to solve Hartree Fock equations self-consistently. Firstly, the single particle states have to be selected. Then, one can compute the mean field Hamiltonian. New single particle states are found by diagonalizing the Hamiltonian. This procedure is repeated until the convergence is realized (Lacroix, 2011, P.16).

The potential and parameters in the expression of the potential are determined by comparing theoretical calculations with experimental data [29]. It is essential to phenomenologically treat a system consisting of many bodies, due to the non-linear growth of the potential for these bodies. Therefore, effective interactions are commonly used within Hartree Fock mean field approximation. The effective NN interaction can be defined as the potential of a long-range part of two-body interaction in the medium of NM [39]. The two common distinguished types of the effective interaction, which are extensively employed, are Skyrme effective interaction and Gogny effective interaction. In this work, we concentrated on the calculations with the Skyrme interaction. The results obtained with Skyrme interactions are compared with results from Gogny interaction.

3.2 Skyrme Effective Interaction

The Skyrme effective interaction is a density-dependent zero-range effective interaction. Initially, it was suggested by Vautherin and Brink [40]. It can be written in terms of a two-body and a three-body parts as cited in [41]. The standard expression of the Skyrme force of the two-body part can be written as [42],

$$\begin{aligned}
V_{ij}^{NN} = & t_o(1 + x_o P_{S_{ij}})\delta(r_i - r_j) \\
& + \frac{1}{2}t_1(1 + x_1 P_{S_{ij}}) \times [\overleftarrow{K}_{ij}^2 \delta(r_i - r_j) + \delta(r_i - r_j) \overrightarrow{K}_{ij}^2] \\
& + t_2(1 + x_2 P_{S_{ij}})[\overleftarrow{K}_{ij} \delta(r_i - r_j) \overrightarrow{K}_{ij}] \\
& + \frac{1}{6}t_3(1 + x_3 P_{S_{ij}})\rho^\sigma \left(\frac{r_i + r_j}{2}\right) \delta(r_i - r_j) \\
& + iW_o \overleftarrow{K}_{ij} \delta(r_i - r_j) (\overrightarrow{S}_i + \overrightarrow{S}_j) \times \overrightarrow{K}_{ij},
\end{aligned} \tag{3.7}$$

where ρ is the nucleon density, and t_i, x_i, σ and W_o are the Skyrme interaction parameters which describe the strengths of these interaction terms [41] and can be found by fitting experimental data. The values of these parameters are recorded in Table 1. $P_{S_{ij}} = (1 + \overrightarrow{S}_i \cdot \overrightarrow{S}_j)/2$ is the operator of spin exchange. \overrightarrow{S}_i is Pauli spin operator and \overrightarrow{K}_{ij} and \overleftarrow{K}_{ij} are the momentum operators. $\overrightarrow{K}_{ij} = -i(\overrightarrow{\nabla}_i - \overrightarrow{\nabla}_j)/2$ operates on the wave functions to the right, and $\overleftarrow{K}_{ij} = i(\overleftarrow{\nabla}_i - \overleftarrow{\nabla}_j)/2$ operates to the left. The zero term t_o represents the central potential, and t_1 and t_2 are non-local terms [40].

Table 1: The parameters for different versions of Skyrme interaction. The values are taken from Ref.[24].

Force	$t_o(\text{MeV fm}^3)$	$t_1(\text{MeV fm}^5)$	$t_2(\text{MeV fm}^5)$	$t_3(\text{MeV fm}^{(3+3\sigma)})$	σ
SKI	-1057.3	235.9	-100	14463.5	1
SKII	-1169.9	585.6	-27.1	9331.1	1
SKIII	-1128.75	395	-95	14000	1
SKIV	-1205.6	765	35	5000	1
SKV	-1248.29	970.56	107.22	0	1

3.3 Gogny Effective Interaction

The Gogny interaction is composed of a set of density-independent finite-range terms in addition to the zero-range terms [43]. It has been widely used in the calculation of the HF mean field as well as the pairing field in NM and nuclei [42]. It has the form [44]

$$\begin{aligned}
V_{ij}^{NN} = & \sum_{ij} (W_i + B_i P_{ij}^s - H_i P_{ij}^\tau - M_i P_{ij}^s P_{ij}^\tau) \exp[-(r_i - r_j)^2 / \mu_i^2] \\
& + t_o (1 + x_o P_{ij}^s) \rho^\sigma \delta(r_i - r_j) \\
& + i W_{LS} (S_i + S_j) \cdot \vec{\nabla} \times \delta(r_i - r_j) \vec{\nabla},
\end{aligned} \tag{3.8}$$

where ρ is the nucleon density, and W_i , B_i , H_i , M_i , t_o , x_o , σ and W_{LS} are parameters. The values of these parameters for D1 interaction are listed in Table 2.

The first part in Eq.(3.8) corresponds to the finite-range interaction, and the second term is the zero-rang term [2]. The spin-orbit contribution introduced as the last term is similar to that of Skyrme expression [45].

Table 2: The parameters of Gogny D1 effective interaction. The values are taken from Ref.[2].

Body	$\mu_i(fm)$	$W_i(MeV)$	$B_i(MeV)$	$H_i(MeV)$	$M_i(MeV)$
1	0.7	-402.4	-100	-496.2	-23.56
2	1.2	-21.3	-11.77	37.24	-68.81

$t_o = 1350 MeV \cdot fm^4, \sigma = 1/3, W_{LS} = 115 MeV \cdot fm^5, x_o = 1.$

3.4 Skyrme Hartree Fock Equations

The Skyrme effective interaction has been widely employed in the study of properties of nuclear matter and nucleus [46]. As it was pointed out in [29] that the total energy (E) for nucleus is given by

$$\begin{aligned} E &= \langle \Phi | H | \Phi \rangle = \langle \Phi | T + \frac{1}{2} \sum_{ij}^N (V_{ij} + V_c) | \Phi \rangle \\ &= \int dr H(r) = \int dr [H_{kin}(r) + H_c(r) + H_{sky}(r)]. \end{aligned} \quad (3.9)$$

The kinetic energy density is given by

$$H_{kin}(r) = \frac{\hbar^2 k^2}{2} \left[\frac{1}{m_p} + \frac{1}{m_n} \right], \quad (3.10)$$

where m_p and m_n are the masses for the proton and neutron, respectively.

The coulomb potential is known as a long-range interaction, which will give a divergence in the result if it is inserted directly in the matrix calculation of plane wave functions. Therefore, a phenomenological expression of coulomb potential is used to simplify the calculations [2].

The average coulomb energy per proton in a uniform charged sphere is given by

$$H_c(r) = aZ^2 \left[1 - 5 \left(\frac{3}{16\pi Z} \right)^{\frac{2}{3}} - \frac{1}{Z} \right] A^{-\frac{4}{3}} \rho^{\frac{1}{3}}, \quad (3.11)$$

where $a = 1.50$ [2].

The total Hamiltonian can be expressed as a summation of different terms

$$H_{sky} = H_o + H_3 + H_{m*} + H_{finite} + H_{s-o} + H_{s-g}, \quad (3.12)$$

where the H_o is the zero-range term, H_3 denotes the density-dependent term, H_{m*} is the effective mass term, H_{finite} corresponds to a finite term, the spin-orbit term is H_{s-o} , and the tensor term H_{s-g} is resulted from the tensor coupling with spin and gradient. We can

get the expression of these terms by evaluating H_{sky} as

$$H_{sky} = \frac{1}{2} \sum \int dr_1 dr_2 dr'_1 dr'_2 \varphi_i^*(r'_1) \varphi_j^*(r'_2) V_{sky}(r_1, r_2) (1 - \hat{P}_r \hat{P}_s \hat{P}_\tau) \varphi_i(r_1) \varphi_j(r_2), \quad (3.13)$$

where P_r , P_s and P_τ are the exchange operators for position, spin and isospin, respectively. The value of position operator, P_r , depends on the power of momentum operator K and it equals 1 or -1 according to the momentum power being odd or even, respectively. The isospin exchange operator, P_τ , yields $\delta_{\tau_1 \tau_2}$, where $\tau_i = \frac{1}{2}$ for a proton and $\tau_i = -\frac{1}{2}$ for a neutron. The reason for considering the isospin is owing to the postulate that says there is no charge mixing in HF states. The exchange operator value of spin has been previously mentioned.

Without symmetry constraints or any further suppositions, the Skyrme force terms are evaluated and expressed as illustrated in [29, 40, 47], and some useful identities are given in Appendix A.

3.4.1 The Zero-Range Term

The zero-range or central term is proportional to t_o in the Skyrme force formalism Eq.(3.7), given by $t_o(1 + x_o \hat{P}_{ij}^s) \delta(r_i - r_j)$. Inserting it in Eq.(3.13), with $P_r = 1$, we will have

$$\int H_o(r) dr = \frac{1}{2} \sum_{ij}^N \langle ij | t_o (1 + x_o \hat{P}_{12}^s) \delta(r_i - r_j) (1 - \hat{P}_{12}^r \hat{P}_{12}^s \hat{P}_{12}^\tau) | ij \rangle, \quad (3.14)$$

where

$$(1 + x_o \hat{P}_{12}^s) (1 - \hat{P}_{12}^r \hat{P}_{12}^s \hat{P}_{12}^\tau) = 1 + \frac{1}{2} (x_o - \delta_{\tau_1 \tau_2}) (1 + \vec{S}_1 \cdot \vec{S}_2) - x_o \delta_{\tau_1 \tau_2}. \quad (3.15)$$

We also have

$$\int H_o(r) dr = \frac{t_o}{2} \sum_{ij}^N \langle ij | \delta(r_1 - r_2) (1 + \frac{1}{2} (x_o - \delta_{\tau_1 \tau_2}) (1 + \vec{S}_1 \cdot \vec{S}_2) - (x_o - \delta_{\tau_1 \tau_2})) | ij \rangle. \quad (3.16)$$

Using the following identities

$$\begin{aligned} \sum_{ij}^N \langle ij | \delta(r_1 - r_2) | ij \rangle &= \sum_{ij}^N \int dr_1 dr_2 \varphi_i^*(r_1) \varphi_j^*(r_2) \delta(r_1 - r_2) \varphi_i(r_1) \varphi_j(r_2) \\ &= \sum_{ij}^N \int dr_1 \varphi_i^*(r_1) \varphi_j^*(r_1) \varphi_i(r_1) \varphi_j(r_1) = \int \rho^2 dr, \end{aligned} \quad (3.17)$$

$$\sum_{ij}^N \langle ij | \delta(r_1 - r_2) \delta_{\tau_1 \tau_2} | ij \rangle = \int (\rho_n^2 - \rho_p^2) dr, \quad (3.18)$$

and

$$\sum_{ij}^N \langle ij | \delta(r_1 - r_2) \vec{S}_i \vec{S}_j | ij \rangle = \sum_{ij}^N \langle ij | \delta(r_1 - r_2) \vec{S}_i \vec{S}_j \delta_{\tau_1 \tau_2} | ij \rangle = 0, \quad (3.19)$$

one has

$$\begin{aligned} \int H_o(r) dr &= \frac{t_o}{2} \sum_{ij} \langle ij | \delta(r_1 - r_2) | ij \rangle \\ &\quad - \frac{t_o}{2} \sum_{ij} \langle ij | x_o \delta(r_1 - r_2) \delta_{\tau_1 \tau_2} | ij \rangle \\ &\quad + \frac{t_o}{4} \sum_{ij} \langle ij | (x_o - \delta_{\tau_1 \tau_2}) \delta(r_1 - r_2) (1 + \vec{S}_1 \vec{S}_2) | ij \rangle. \end{aligned} \quad (3.20)$$

Thus one has

$$\begin{aligned} \int H_o(r) dr &= \int \left(\frac{1}{2} t_o \rho^2 - \frac{1}{2} t_o x_o (\rho_n^2 + \rho_p^2) + \frac{1}{4} t_o x_o \rho^2 - \frac{1}{4} t_o (\rho_n^2 + \rho_p^2) \right) dr \\ &= \int \frac{1}{4} t_o [\rho^2 (2 + x_o) - (\rho_n^2 + \rho_p^2) (2x_o + 1)]. \end{aligned} \quad (3.21)$$

3.4.2 The Density Dependence Term

The density dependence term, the term proportional to t_3 in Eq.(3.7), is important in describing a finite nucleus [34]. Its expression can be derived in a similar way as t_o ,

$$(1 + x_3 \hat{P}_{12}^s)(1 - \hat{P}_{12}^r \hat{P}_{12}^s \hat{P}_{12}^\tau) = 1 + \frac{x_3}{2} - \frac{1}{2} \delta_{\tau_1 \tau_2} + \frac{x_3}{2} \vec{S}_1 \vec{S}_2 - \frac{1}{2} \delta_{\tau_1 \tau_2} \vec{S}_1 \vec{S}_2 - x_3 \delta_{\tau_1 \tau_2}. \quad (3.22)$$

$$\begin{aligned}
\int H_3(r)dr &= \frac{t_3}{2} \sum_{ij} \langle ij | \frac{1}{6} (1 + x_3 \hat{P}_{ij}^s) \rho^\sigma \left(\frac{r_i - r_j}{2} \right) \delta(r_i - r_j) (1 - \hat{P}_{12}^r \hat{P}_{12}^s \hat{P}_{12}^r) | ij \rangle \\
&= \frac{t_3}{12} (1 + \frac{x_3}{2}) \sum_{ij} \langle ij | \rho^\sigma \left(\frac{r_i - r_j}{2} \right) \delta(r_i - r_j) | ij \rangle \\
&\quad - \frac{t_3}{24} \sum_{ij} \langle ij | \rho^\sigma \left(\frac{r_i - r_j}{2} \right) \delta(r_i - r_j) \delta_{\tau_1 \tau_2} | ij \rangle \\
&\quad + \frac{t_3}{24} x_3 \sum_{ij} \langle ij | \rho^\sigma \left(\frac{r_i - r_j}{2} \right) \delta(r_i - r_j) \vec{S}_1 \vec{S}_2 | ij \rangle \\
&\quad - \frac{t_3}{24} \sum_{ij} \langle ij | \rho^\sigma \left(\frac{r_i - r_j}{2} \right) \delta(r_i - r_j) \vec{S}_1 \vec{S}_2 \delta_{\tau_1 \tau_2} | ij \rangle \\
&\quad - \frac{t_3}{12} x_3 \sum_{ij} \langle ij | \rho^\sigma \left(\frac{r_i - r_j}{2} \right) \delta(r_i - r_j) \delta_{\tau_1 \tau_2} | ij \rangle.
\end{aligned} \tag{3.23}$$

The final form for the density dependence term is

$$H_3(r) = \frac{t_3}{12} \rho^\sigma \left[\rho^2 (1 + \frac{x_3}{2}) - (\frac{1}{2} + x_3) (\rho_n^2 + \rho_p^2) \right]. \tag{3.24}$$

3.4.3 The Momentum Dependence Term

We start with t_1 term

$$\frac{t_1}{2} (1 + x_1 \hat{P}_{ij}^s) [\overleftarrow{K}_{ij}^2 + \overrightarrow{K}_{ij}^2] \delta(r_i - r_j). \tag{3.25}$$

We have

$$\overleftarrow{K}_{ij}^2 + \overrightarrow{K}_{ij}^2 = -\frac{1}{4} [\overrightarrow{\nabla}_1^2 + \overrightarrow{\nabla}_2^2 + \overleftarrow{\nabla}_1^2 + \overleftarrow{\nabla}_2^2 - 2\overrightarrow{\nabla}_1 \overrightarrow{\nabla}_2 - 2\overleftarrow{\nabla}_1 \overleftarrow{\nabla}_2], \tag{3.26}$$

and

$$\begin{aligned}
\overrightarrow{\nabla}^2 \rho &= \sum_i \overrightarrow{\nabla} [\overrightarrow{\nabla} \varphi_i^*(r) \varphi_i(r) + \varphi_i^* \overrightarrow{\nabla} \varphi_i(r)] \\
&= \sum_i [\overrightarrow{\nabla}^2 \varphi_i^*(r) \varphi_i(r) + 2\overrightarrow{\nabla} \varphi_i^*(r) \overrightarrow{\nabla} \varphi_i(r) + \varphi_i^*(r) \overrightarrow{\nabla}^2 \varphi_i(r)] \\
&= 2\tau + 2 \sum_i \overrightarrow{\nabla}^2 \varphi_i^*(r) \varphi_i(r).
\end{aligned} \tag{3.27}$$

Thus, we have

$$\vec{\nabla}^2 \varphi_i^*(r) \varphi_i(r) = \varphi_i^*(r) \vec{\nabla}^2 \varphi_i(r) = -\tau + \frac{1}{2} \vec{\nabla}^2 \rho, \quad (3.28)$$

and

$$\sum_{ij} \langle ij | \delta(r_1 - r_2) \vec{\nabla}_1^2 | ij \rangle = \int (-\tau \rho + \frac{1}{2} \rho \vec{\nabla}^2 \rho) dr, \quad (3.29)$$

where $\vec{\nabla}_1^2 = \vec{\nabla}_2^2 = \overleftarrow{\nabla}_1^2 = \overleftarrow{\nabla}_2^2$.

We have

$$\sum_{ij} \langle ij | \delta(r_1 - r_2) \vec{\nabla}_1^2 \delta_{\tau_1 \tau_2} | ij \rangle = \int [-\tau_n \rho_n - \tau_p \rho_p + \frac{1}{2} \rho_n \vec{\nabla}^2 \rho_n + \frac{1}{2} \rho_p \vec{\nabla}^2 \rho_p] dr, \quad (3.30)$$

and

$$\begin{aligned} \sum_{ij} \langle ij | \delta(r_1 - r_2) \vec{\nabla}_1 \vec{\nabla}_2 | ij \rangle &= \sum_{ij} \int dr_1 dr_2 \varphi_i^*(r_1) \vec{\nabla} \varphi_i(r_1) \varphi_j^*(r_2) \vec{\nabla} \varphi_j(r_2) \delta(r_1 - r_2) \\ &= \sum_{ij} \int dr_1 \varphi_i^*(r_1) \vec{\nabla} \varphi_i(r_1) \int dr_2 \varphi_j^*(r_2) \vec{\nabla} \varphi_j(r_2) \delta(r_1 - r_2) \\ &= \sum_{ij} \left(- \int dr_1 \vec{\nabla} \varphi_i^*(r_1) \varphi_i(r_1) \right) \left(- \int dr_2 \vec{\nabla} \varphi_j^*(r_2) \varphi_j(r_2) \delta(r_1 - r_2) \right) \\ &= \frac{1}{4} \int dr (\vec{\nabla} \rho)^2, \end{aligned} \quad (3.31)$$

and

$$\sum_{ij} \langle ij | \delta(r_1 - r_2) \vec{\nabla}_1 \vec{\nabla}_2 \delta_{\tau_1 \tau_2} | ij \rangle = \frac{1}{4} \int d^3 r [(\vec{\nabla} \rho_n)^2 + (\vec{\nabla} \rho_p)^2], \quad (3.32)$$

we have the identity

$$(\vec{\nabla}_1 \vec{\nabla}_2)(\vec{S}_1 \vec{S}_2) = \frac{1}{3} (\vec{\nabla}_1 \vec{S}_1)(\vec{\nabla}_2 \vec{S}_2) + \frac{1}{2} (\vec{\nabla}_1 \times \vec{S}_1)(\vec{\nabla}_2 \times \vec{S}_2) + (\vec{\nabla}_1 \times \vec{S}_1)^{(2)} (\vec{\nabla}_2 \times \vec{S}_2)^{(2)}. \quad (3.33)$$

With the assumption of symmetry and invariance of time reversal, we have

$$\sum_i \varphi_i^*(r) (\vec{\nabla} \vec{S}) \varphi_i(r) = \sum_i \varphi_i^*(r) (\vec{\nabla} \times \vec{S})^{(2)} \varphi_i(r) = 0. \quad (3.34)$$

Hence

$$\begin{aligned}
& \sum_{ij} \langle ij | \delta(r_1 - r_2) (\vec{\nabla}_1 \vec{\nabla}_2) (\vec{S}_1 \vec{S}_2) | ij \rangle \\
&= \frac{1}{2} \sum_{ij} \int dr_1 dr_2 \delta(r_1 - r_2) \varphi_i^*(r_1) (\vec{\nabla}_1 \times \vec{S}_1) \varphi_i(r_1) \varphi_j^*(r_2) (\vec{\nabla}_2 \times \vec{S}_2) \varphi_j(r_2) \\
&= -\frac{1}{2} \int J^2 dr,
\end{aligned} \tag{3.35}$$

where

$$-i \sum_i \varphi_i^*(r) (\vec{\nabla}_i \times \vec{S}_i) \varphi_i(r) = J(r), \tag{3.36}$$

and

$$\sum_{ij} \langle ij | \delta(r_1 - r_2) (\vec{\nabla}_1 \vec{\nabla}_2) (\vec{S}_1 \vec{S}_2) \delta_{\tau_1 \tau_2} | ij \rangle = -\frac{1}{2} \int dr (J_n^2 + J_p^2). \tag{3.37}$$

With

$$(1 + x_1 \hat{P}_{12}^s) (1 - \hat{P}_{12}^r \hat{P}_{12}^s \hat{P}_{12}^\tau) = 1 + \frac{1}{2} (x_1 - \delta_{\tau_1 \tau_2}) (1 + \vec{S}_1 \cdot \vec{S}_2) - x_1 \delta_{\tau_1 \tau_2}, \tag{3.38}$$

we get

$$\begin{aligned}
\int H_1(r) dr &= \frac{1}{2} \sum_{ij} \langle ij | \frac{t_1}{2} (1 + x_1 \hat{P}_{ij}^s) \delta(r_i - r_j) [\hat{K}_{ij}^2 + \bar{K}_{ij}^2] (1 - \hat{P}_{12}^r \hat{P}_{12}^s \hat{P}_{12}^\tau) | ij \rangle \\
&= \sum_{ij} \langle ij | -\frac{t_1}{16} \delta(r_i - r_j) [\hat{K}_{ij}^2 + \bar{K}_{ij}^2] | ij \rangle \\
&+ \sum_{ij} \langle ij | -\frac{t_1}{32} \delta(r_i - r_j) (x_1 - \delta_{\tau_1 \tau_2}) [\hat{K}_{ij}^2 + \bar{K}_{ij}^2] (1 + \vec{S}_1 \vec{S}_2) | ij \rangle \\
&+ \sum_{ij} \langle ij | -\frac{t_1}{16} x_1 \delta(r_i - r_j) \delta_{\tau_1 \tau_2} [\hat{K}_{ij}^2 + \bar{K}_{ij}^2] | ij \rangle.
\end{aligned} \tag{3.39}$$

Thus we have

$$\begin{aligned}
\int H_1(r) dr &= \frac{t_1}{16} \int dr (4\tau\rho - 2\rho \vec{\nabla}^2 \rho + (\vec{\nabla} \rho)^2) \\
&- \frac{t_1}{16} x_1 \int dr (-2\tau\rho + 2\rho \vec{\nabla}^2 \rho - \frac{1}{2} (\vec{\nabla} \rho)^2) - \frac{t_1}{16} \int x_1 J^2 dr \\
&- \frac{t_1}{16} x_1 \int dr (-2\tau_n \rho_n - 2\tau_p \rho_p + \rho_n \vec{\nabla}^2 \rho_n + \rho_p \vec{\nabla}^2 \rho_p) \\
&- \frac{t_1}{32} \int dr [(\vec{\nabla} \rho_n)^2 + (\vec{\nabla} \rho_p)^2] + \frac{t_1}{16} \int (J_n^2 + J_p^2) dr \\
&- \frac{t_1}{16} x_1 \int dr (-4\tau_n \rho_n - 4\tau_p \rho_p + 2\rho_n \vec{\nabla}^2 \rho_n + 2\rho_p \vec{\nabla}^2 \rho_p) \\
&- \frac{t_1}{16} x_1 \int dr [(\vec{\nabla} \rho_n)^2 + (\vec{\nabla} \rho_p)^2].
\end{aligned} \tag{3.40}$$

Finally, we obtain

$$\begin{aligned}
H_1(r) &= \frac{t_1}{16} \left(1 + \frac{x_1}{2}\right) [4\tau\rho - 3\rho\vec{\nabla}^2\rho] \\
&\quad - \frac{t_1}{16} \left(\frac{1}{2} + x\right) [4\tau_n\rho_n + 4\tau_p\rho_p - 3\rho_n\vec{\nabla}^2\rho_n - 3\rho_p\vec{\nabla}^2\rho_p] \\
&\quad + \frac{t_1}{16} (-x_1J^2 + J_n^2 + J_p^2).
\end{aligned} \tag{3.41}$$

Now we move to t_2 term

$$[t_2(1 + x_2\hat{P}_{ij}^s)\overleftarrow{K}_{ij}\delta(r_1 - r_2)\overrightarrow{K}_{ij}]. \tag{3.42}$$

We have to find

$$\int H_2(r)dr = \frac{1}{2} \sum_{ij} \langle ij | t_2(1 + x_2\hat{P}_{ij}^s)\overleftarrow{K}_{ij}\delta(r_1 - r_2)\overrightarrow{K}_{ij}(1 - \hat{P}_{12}^r\hat{P}_{12}^s\hat{P}_{12}^\tau) | ij \rangle. \tag{3.43}$$

In this case where the momentum power is odd, the position exchange operator, $\hat{P}_{12}^r = -1$, we get

$$\hat{P}_{12}^r\hat{P}_{12}^s\hat{P}_{12}^\tau = -\frac{1}{2}(1 + \vec{S}_1\vec{S}_2)\delta_{\tau_1\tau_2}.$$

Therefore

$$(1 + x_2\hat{P}_{ij}^s)(\hat{P}_{12}^r\hat{P}_{12}^s\hat{P}_{12}^\tau) = 1 + \frac{x_2}{2} + \frac{1}{2}(x_2 + \delta_{\tau_1\tau_2})\vec{S}_1\vec{S}_2 + \left(\frac{1}{2} + x_2\right)\delta_{\tau_1\tau_2}. \tag{3.44}$$

We use the processes as in term t_1 in addition to the following expression,

$$\overrightarrow{K}_{ij}\overleftarrow{K}_{ij} = \frac{1}{4} \left[\overrightarrow{\nabla}_i\overleftarrow{\nabla}_i + \overrightarrow{\nabla}_j\overleftarrow{\nabla}_j - \overrightarrow{\nabla}_i\overleftarrow{\nabla}_j - \overrightarrow{\nabla}_j\overleftarrow{\nabla}_i \right]. \tag{3.45}$$

We have

$$\begin{aligned}
\int H_2(r)dr &= \frac{1}{2} \sum_{ij} \langle ij | t_2(1 + x_2\hat{P}_{ij}^s)\overleftarrow{K}_{ij}\delta(r_1 - r_2)\overrightarrow{K}_{ij}(1 - \hat{P}_{12}^r\hat{P}_{12}^s\hat{P}_{12}^\tau) | ij \rangle \\
&= \frac{t_2}{2} \left(1 + \frac{x_2}{2}\right) \sum_{ij} \langle ij | \overleftarrow{K}_{ij}\overrightarrow{K}_{ij}\delta(r_1 - r_2) | ij \rangle \\
&\quad + \frac{t_2}{2} \left(\frac{1}{2} + x_2\right) \sum_{ij} \langle ij | \overleftarrow{K}_{ij}\overrightarrow{K}_{ij}\delta(r_1 - r_2)\delta_{\tau_1\tau_2} | ij \rangle \\
&\quad + \frac{t_2}{4} x_2 \langle ij | \overleftarrow{K}_{ij}\overrightarrow{K}_{ij}\delta(r_1 - r_2)\vec{S}_1\vec{S}_2 | ij \rangle \\
&\quad + \frac{t_2}{4} \langle ij | \overleftarrow{K}_{ij}\overrightarrow{K}_{ij}\delta(r_1 - r_2)\vec{S}_1\vec{S}_2\delta_{\tau_1\tau_2} | ij \rangle.
\end{aligned} \tag{3.46}$$

Then, we have

$$\begin{aligned}
H_2(r) &= \frac{t_2}{16}(2+x_2)(2\tau\rho + \frac{1}{2}\rho\vec{\nabla}^2\rho) \\
&+ \frac{t_2}{16}(1+2x_2)(2\tau_n\rho_n + 2\tau_p\rho_p + \frac{1}{2}\rho_n\vec{\nabla}^2\rho_n + \frac{1}{2}\rho_p\vec{\nabla}^2\rho_p) \\
&- \frac{t_2}{16}(x_2J^2 + J_n^2 + J_p^2).
\end{aligned} \tag{3.47}$$

3.4.4 The Spin-Orbit Term

The spin-orbit term is proposed originally by Bell and Skyrme [48], and within the mean field method, it gives rise to the potential of one-body [49]. The contribution from this term only appears with triplet states where $\hat{P}_{12}^r = -1, \hat{P}_{12}^s = 1$.

To calculate

$$\int H_{s-o}(r)dr = \frac{1}{2} \sum_{ij} \langle ij | iW_o \overleftarrow{K}_{ij} \delta(r_i - r_j) (\vec{S}_i + \vec{S}_j) \times \overrightarrow{K}_{ij} (1 - \hat{P}_{12}^r \hat{P}_{12}^s \hat{P}_{12}^t) | ij \rangle, \tag{3.48}$$

we use the following results

$$\overleftarrow{K}_{ij} \times \overrightarrow{K}_{ij} = \frac{1}{4} (\overleftarrow{\nabla}_i \times \overrightarrow{\nabla}_i \overleftarrow{\nabla}_j \times \overrightarrow{\nabla}_j - \overleftarrow{\nabla}_j \times \overrightarrow{\nabla}_j \overleftarrow{\nabla}_i \times \overrightarrow{\nabla}_i), \tag{3.49}$$

and

$$\begin{aligned}
4(\vec{S}_i + \vec{S}_j) \overleftarrow{K}_{ij} \times \overrightarrow{K}_{ij} &= \vec{S}_i (\overleftarrow{\nabla}_i \times \overrightarrow{\nabla}_i) + \vec{S}_i (\overleftarrow{\nabla}_j \times \overrightarrow{\nabla}_j) - \vec{S}_i (\overleftarrow{\nabla}_j \times \overrightarrow{\nabla}_i) \\
&- \vec{S}_i (\overleftarrow{\nabla}_i \times \overrightarrow{\nabla}_j) + \vec{S}_j (\overleftarrow{\nabla}_i \times \overrightarrow{\nabla}_i) + \vec{S}_j (\overleftarrow{\nabla}_j \times \overrightarrow{\nabla}_j) \\
&- \vec{S}_j (\overleftarrow{\nabla}_j \times \overrightarrow{\nabla}_i) + \vec{S}_j (\overleftarrow{\nabla}_i \times \overrightarrow{\nabla}_j) \\
&= 2\vec{S}_i (\overleftarrow{\nabla}_i \times \overrightarrow{\nabla}_i) + 2\vec{S}_i (\overleftarrow{\nabla}_j \times \overrightarrow{\nabla}_j) \\
&- 2\vec{S}_i (\overleftarrow{\nabla}_j \times \overrightarrow{\nabla}_i + \overleftarrow{\nabla}_i \times \overrightarrow{\nabla}_j).
\end{aligned} \tag{3.50}$$

Thus we have

$$\begin{aligned}
\int H_{s-o}(r)dr &= \frac{iW_o}{4} \sum_{ij} \langle ij | \delta(r_i - r_j) \vec{S}_i (\vec{\nabla}_i \times \vec{\nabla}_i) (1 + \delta_{\tau_i \tau_j}) | ij \rangle \\
&+ \frac{iW_o}{4} \sum_{ij} \langle ij | \delta(r_i - r_j) \vec{S}_i (\vec{\nabla}_j \times \vec{\nabla}_j) (1 + \delta_{\tau_i \tau_j}) | ij \rangle \\
&- \frac{iW_o}{4} \sum_{ij} \langle ij | \delta(r_i - r_j) \vec{S}_i (\vec{\nabla}_i \times \vec{\nabla}_j) (1 + \delta_{\tau_i \tau_j}) | ij \rangle \\
&- \frac{iW_o}{4} \sum_{ij} \langle ij | \delta(r_i - r_j) \vec{S}_i (\vec{\nabla}_j \times \vec{\nabla}_i) (1 + \delta_{\tau_i \tau_j}) | ij \rangle.
\end{aligned} \tag{3.51}$$

The contribution of the second term will vanish, and also we have

$$\begin{aligned}
\vec{S}_i (\vec{\nabla}_i \times \vec{\nabla}_i) &= -2\vec{\nabla}_j (\vec{\nabla}_i \times \vec{S}_i) \\
-\vec{S}_i (\vec{\nabla}_i \times \vec{\nabla}_j) &= -\vec{\nabla}_j (\vec{\nabla}_i \times \vec{S}_i) \\
\vec{S}_i (\vec{\nabla}_j \times \vec{\nabla}_i) &= \vec{\nabla}_j (\vec{\nabla}_i \times \vec{S}_i).
\end{aligned} \tag{3.52}$$

Therefore, we have

$$\begin{aligned}
\int H_{s-o}(r)dr &= -iW_o \sum_{ij} \langle ij | \delta(r_i - r_j) (1 + \delta_{\tau_i \tau_j}) \vec{\nabla}_j (\vec{\nabla}_i \times \vec{S}_i) | ij \rangle \\
&= -iW_o \sum_{ij} \int dr_1 dr_2 \delta(r_i - r_j) (1 + \delta_{\tau_i \tau_j}) \varphi_j^* \vec{\nabla}_j \varphi_j \varphi_i^* (\vec{\nabla}_i \times \vec{S}_i) \varphi_i \\
&= \frac{W_o}{2} \int dr (\vec{\nabla} \rho J + \vec{\nabla} \rho_n J_n + \vec{\nabla} \rho_p J_p) \\
&= -\frac{W_o}{2} \int dr (\rho \vec{\nabla} J + \rho_n \vec{\nabla} J_n + \rho_p \vec{\nabla} J_p).
\end{aligned} \tag{3.53}$$

The final expression of Skyrme energy density can be written as

$$\begin{aligned}
H_{sky}(r) = & \frac{t_o}{4} [\rho^2(2 + x_o) - (\rho_n^2 + \rho_p^2)(2x_o + 1)] \\
& + \frac{t_1}{16} (1 + \frac{x_1}{2}) [4\tau\rho - 3\rho\vec{\nabla}^2\rho] \\
& - \frac{t_1}{16} (\frac{1}{2} + x_1) [4\tau_n\rho_n + 4\tau_p\rho_p - 3\rho_n\vec{\nabla}^2\rho_n - 3\rho_p\vec{\nabla}^2\rho_p] \\
& + \frac{t_1}{16} (-x_1J^2 + J_n^2 + J_p^2) + \frac{t_2}{16} (2 + x_2) (2\tau\rho + \frac{1}{2}\rho\vec{\nabla}^2\rho) \\
& + \frac{t_2}{16} (1 + 2x_2) [2\tau_n\rho_n + 2\tau_p\rho_p + \frac{1}{2}\rho_n\vec{\nabla}^2\rho_n + \frac{1}{2}\rho_p\vec{\nabla}^2\rho_p] \\
& - \frac{t_2}{16} (x_2J^2 + J_n^2 + J_p^2) + \frac{t_3}{12}\rho^\sigma [\rho^2(1 + \frac{x_3}{2}) - (\frac{1}{2} + x_3)(\rho_n^2 + \rho_p^2)] \\
& - \frac{W_o}{2} \int dr (\rho\vec{\nabla}J + \rho_n\vec{\nabla}J_n + \rho_p\vec{\nabla}J_p).
\end{aligned} \tag{3.54}$$

To make it more explicit, we can express each term in Eq.(3.54) as follows,

$$H_o(r) = \frac{t_o}{4} [\rho^2(2 + x_o) - (\rho_n^2 + \rho_p^2)(2x_o + 1)], \tag{3.55}$$

$$H_3(r) = \frac{t_3}{24}\rho^\sigma [\rho^2(2 + x_3) - (1 + 2x_3)(\rho_n^2 + \rho_p^2)], \tag{3.56}$$

$$H_{m^*}(r) = \frac{1}{8} [t_1(2 + x_1) + t_2(2 + x_2)]\tau\rho + \frac{1}{8} [t_2(1 + 2x_2) - t_1(1 + 2x_1)], \tag{3.57}$$

$$\begin{aligned}
H_{finite}(r) = & \frac{1}{32} [3t_1(2 + x_1) - t_2(2 + x_2)] (\vec{\nabla}\rho)^2 \\
& - \frac{1}{32} [3t_1(2x_1 + 1) + t_2(2x_2 + 1)] [(\vec{\nabla}\rho_n)^2 + (\vec{\nabla}\rho_p)^2],
\end{aligned} \tag{3.58}$$

$$H_{s-o}(r) = \frac{W_o}{2} [J \cdot \vec{\nabla}\rho + J_n \cdot \vec{\nabla}\rho_n + J_p \cdot \vec{\nabla}\rho_p], \tag{3.59}$$

$$H_{s-g}(r) = -\frac{1}{16} (t_1x_1 + t_2x_2)J^2 + \frac{1}{16} (t_1 - t_2) [J_n^2 + J_p^2], \tag{3.60}$$

where the nucleon density $\rho(r) = \rho_p(r) + \rho_n(r)$, the kinetic energy $\tau(r)$, and the current densities $J(r)$, are given by

$$\rho(r) = \sum_{is} \varphi_i^*(r, s, \tau) \varphi_i(r, s, \tau), \quad (3.61)$$

$$\tau(r) = \sum_{is} \vec{\nabla} \varphi_i^*(r, s, \tau) \vec{\nabla} \varphi_i(r, s, \tau), \quad (3.62)$$

and

$$J(r) = -i \sum_{iss'} \varphi_i^*(r, s, \tau) \left[\vec{\nabla} \sum_{is} \varphi_i(r, s', \tau) \times \langle s | \vec{s} | s' \rangle \right]. \quad (3.63)$$

4 The Equation of State Calculation

This chapter presents the formulism used in the calculation of the Equation of State (EOS) for NM and finite nuclei. Firstly, we described our model with the Skyrme interaction for symmetric nuclear matter and finite nuclei. Then, we calculated the static properties and elucidated how the finite size parameter a_F can be determined. Finally, we described the procedures for deriving the chemical potential and determining the critical temperature.

4.1 The Model Description

The model employed earlier in Ref. [42], has been used in this work with Skyrme effective interaction,

$$\begin{aligned}
 V_{ij}^{NN} = & t_o(1 + x_o P_{S_{ij}})\delta(r_i - r_j) \\
 & + \frac{1}{2}t_1(1 + x_1 P_{S_{ij}}) \times [\overleftarrow{K}_{ij}^2 \delta(r_i - r_j) + \delta(r_i - r_j) \overrightarrow{K}_{ij}^2] \\
 & + t_2(1 + x_2 P_{S_{ij}})[\overleftarrow{K}_{ij} \delta(r_i - r_j) \overrightarrow{K}_{ij}] \\
 & + \frac{1}{6}t_3(1 + x_3 P_{S_{ij}})\rho^\sigma \left(\frac{r_i + r_j}{2}\right) \delta(r_i - r_j) \\
 & + iW_o \overleftarrow{K}_{ij} \delta(r_i - r_j) (\overrightarrow{S}_i + \overrightarrow{S}_j) \times \overrightarrow{K}_{ij}.
 \end{aligned} \tag{4.1}$$

As we shall concentrate on a symmetric case in our calculations, only zero-range and density dependence terms need to be included in Skyrme force Eq.(4.1). Several versions of Skyrme force can be found in literature [50].

In this paper, SKI, SKII, SKIII, SKIV and SKV parameterizations will be employed. The procedure used in our calculations is the self-consistent Hartree Fock approximation¹. It needs to be implemented numerically.

¹This procedure has been illustrated in Chapter 3.

According to HF approximation, the total energy of NM is obtained from the expectation value of Skyrme interaction

$$E(\rho, T) = v \int n(k) \frac{\hbar^2 k^2}{2m} \frac{d^3 k}{(2\pi)^3} + \frac{v^2}{2} \int n(k_1) n(k_2) \frac{d^3 k_1}{(2\pi)^3} \frac{d^3 k_2}{(2\pi)^3} \langle \vec{k}_1 \vec{k}_2 | V_{NN} | \vec{k}_1 \vec{k}_2 \rangle_a, \quad (4.2)$$

where $v = (2s + 1)(2\tau + 1) = 4$ is the factor due to spin and isospin degeneracy, $n(k)$ is the momentum distribution which obeys Fermi-Dirac distribution, and the subscript a indicates that only antisymmetric matrix elements are required.

4.1.1 Symmetric Nuclear Matter

The meaning of symmetric nuclear matter is related to the fact that for each neutron there is a proton (i.e. the system is homogeneous), thereby

$$Z = N = \frac{A}{2},$$

where A is the mass number, Z and N are the proton and neutron number, respectively.

Furthermore, the density, ρ is constant in this system, so that

$$\rho_p = \rho_n = \frac{\rho}{2}.$$

Another property regarding symmetric matter is that there is no spin-polarization, namely, the distribution of the spin being random [51]. In our calculations we can describe the NM as a box with volume V , which tends to infinity. In this case, the effect of the volume is only considered in calculating the energy, without any contribution from the surface term. It is well-known that the wave function of the single particle in an infinite system can be described by a plane wave function. Also, the momentum is fixed due to the fact that the system does not change under translations in the space. So, the total number of nucleons in the system between k and $k + dk$ in the momentum space can be obtained from,

$$dN_k = \frac{V}{2\pi^2} k^2 dk. \quad (4.3)$$

4.1.2 Finite System

This section is devoted to explaining the significant considerations related to the distinguished procedures in the calculations for the infinite and finite systems. In a finite system, we should consider the effect from the finite size which has been emphasized in the work performed by Jagaman et al. [20]. In this work, the model used is a box of a surface S and volume V containing N -nucleons. The finite size effect can be studied approximately with Hill-Wheeler formula,

$$dN_k = V \left[\frac{k^2 dk}{2\pi^2} - \frac{S}{V} \frac{k dk}{8\pi} + \frac{L}{V} \frac{dk}{8\pi} \right]. \quad (4.4)$$

This expression was initially calculated for a cuboid with dimensions a , b , and c . The surface area of the cuboid is S and the linear size is $L = 2a + 2b + 2c$. Generally, it is valid for any regular system, and for a spherical nuclei with radius R , one has $S = 4\pi R^2$ and $L = 2\pi R$.

Ref.[2] pointed out that the simple model used to derive Eq.(4.4) cannot be applied directly to a nucleus, since the wave function of the single particle in finite size system cannot be plane wave function if there are interactions between nucleons. The number of state given in Eq.(4.4) is an approximation in computing dN_k .

It was found [2] that calculations for the zero temperature properties employing Eq.(4.4) for six typical nuclei with Gogny effective interaction do not agree with the experimental results; the calculated binding energies are much smaller than that found experimentally. This difference between the experimental data and the calculated results becomes more serious with the decreasing of nucleon number in the system. This suggests Eq.(4.4) does not include the finite size effect suitably. It is expected that the EOS calculations that have been carried out with Eq.(4.4) are not rigorous.

Cao and Yang introduced a finite size parameter (a_F) in Eq.(4.4) to account for the difference in the wave function between the nucleus and infinite system,

$$dN_k = V \frac{k^2 dk}{2\pi^2} + a_F \left[- \left(\frac{4\pi\rho}{3A} \right)^{\frac{1}{3}} \frac{3k dk}{8\pi} + \left(\frac{4\pi\rho}{3A} \right)^{\frac{2}{3}} \frac{3dk}{16\pi} \right]. \quad (4.5)$$

A value of $a_F = 0.35$ was obtained for calculations with Gogny force. It should be noted that if a_F is taken to be 1, then Eq.(4.5) will become Eq.(4.4), and also become Eq.(4.3) as $N \rightarrow \infty$.

The binding energies calculated in Ref.[2] are listed in Table 3. Our first interest is to determine the value for the parameter of the finite size effect in the calculation with Skyrme force to investigate the dependence on the effective forces employed. Then, we will study the liquid-gas phase transition for nuclear matter and nuclei.

Table 3: The ground state energies for six typical nuclei employing Eq.(4.4) and Gogny interaction found in Ref.[2].

Nuclei	Binding Energy(MeV)		
	Exp.	Eq.(4.5)	Eq.(4.4)
${}_{20}^{40}Ca$	8.55	8.97	-1.01
${}_{28}^{56}Ni$	8.64	8.82	-0.60
${}_{40}^{90}Zr$	8.71	8.72	0.66
${}_{62}^{156}Sm$	8.25	8.02	1.20
${}_{82}^{208}Pb$	7.87	7.45	1.30
${}_{92}^{238}U$	7.57	7.15	1.29

4.2 Zero Temperature Properties

The primary purpose in this part is to study the saturation properties of symmetric NM and nuclei in order to deduce the value of the finite size effect parameter a_F . Therefore, we will consider zero temperature matter which is completely degenerate according to the fermi gas method. In fact, this approximation is a powerful tool for NM where its validity is guaranteed for a wide range of energies.

It is worth pointing out that the single particle² momentum k in a system at zero temperature is below the fermi level. In other words, the energy ε_i is lower than the fermi energy ε_f , and the occupation number n_i of the single particles equals 1 as seen in Fig.6. The saturation density ρ_o can be directly written in terms of fermi momentum k_f

$$\begin{aligned}\rho &= v \int_0^{k_f} \frac{d^3k}{(2\pi)^3} n(k) \\ &= \frac{2}{3\pi^2} k_f^3,\end{aligned}\tag{4.6}$$

where $n(k) = 1$ for $k < k_f$ and zero elsewhere. We should mention that the integration is evaluated over the fermi sphere, i.e. k being from 0 to k_f , and also $\frac{d^3k}{(2\pi)^3}$ is equivalently replaced with dN_k for finite system.

We also can calculate the saturation energy using the same technique. To carry out this calculation, it requires firstly to find the kinetic energy,

$$E_{kin} = v \int_0^{k_f} n(k) \frac{\hbar^2 k^2}{2m} \frac{d^3k}{(2\pi)^3} = \frac{vV k_f^3}{10\pi^2} \frac{\hbar^2 k_f^2}{2m}.\tag{4.7}$$

We can use the definition of the fermi energy

$$\varepsilon_f = \frac{\hbar^2 k_f^2}{2m}.$$

²Note that here, the fermi momentum for the neutron and proton are identical as we consider the NM is symmetric and ignore coulomb interaction.

Also we take advantage from the saturation density Eq.(4.6) where the fermi momentum is

$$k_f^3 = \frac{3\pi^2}{2}\rho.$$

Thus, the kinetic energy per nucleon is

$$E_{kin} = \frac{3}{5}\varepsilon_f. \quad (4.8)$$

Now we move to finding the mean field from

$$u(k) = v \int n(k') \frac{d^3k'}{(2\pi)^3} \langle kk' | V_{NN} | kk' \rangle_a. \quad (4.9)$$

Indeed, for the Skyrme effective interaction, the solution for the HF mean field equations is not very complicated because of the simplicity of its structure. Most significantly, we can note in Eq.(4.9) the mean field does not depend on the temperature. The solution of the mean field can be written as

$$u(k) = \frac{\hbar^2 k^2}{2m} \Delta \rho + \bar{u}(k), \quad (4.10)$$

where the first term depends on the momentum. $\Delta \rho$ can be readily obtained from the effective mass definition,

$$\frac{m^*(\rho)}{m} = \left[1 + \frac{2m}{\hbar^2} \frac{1}{16} (3t_1 + 5t_2 + 4t_2 x_2) \rho \right]^{-1} = \frac{1}{1 + \Delta \rho}. \quad (4.11)$$

Thus

$$\Delta \rho = \frac{2m}{\hbar^2} \frac{1}{16} (3t_1 + 5t_2 + 4t_2 x_2) \rho. \quad (4.12)$$

The second term in Eq.(4.10) amounts to

$$\bar{u}(k) = \frac{3}{4} t_o \rho + \frac{t_3}{16} (\sigma + 1) \rho^{\sigma+1}, \quad (4.13)$$

which includes the contribution from the rearrangement potential that yields

$$\bar{u}_R(k) = \frac{1}{16} \sigma t_3 \rho^{\sigma+1}. \quad (4.14)$$

Such contribution needs to be included in the calculation for the chemical potential. The reason for its importance is that it can guarantee the density relation, $\rho = \frac{1}{V} \sum_k n(k)$ [2].

By integrating Eq.(4.9) from 0 to k_f with the help of Eq.(4.3), and also introducing effective mass, one has³

$$\begin{aligned} u(k) &= \frac{\hbar^2 k_f^2}{2m^*} + \left(\frac{3}{4} t_o \rho + \frac{t_3}{8} \rho^{\sigma+1} \right) \\ &= \frac{\hbar^2 k_f^2}{2m} + \frac{3}{80} (3t_1 + 5t_2 + 4t_2 x_2) \rho k_f^2 + \left(\frac{3}{4} t_o \rho + \frac{t_3}{8} \rho^{\sigma+1} \right). \end{aligned} \quad (4.15)$$

Now one can obtain the ground state energy from Eq.(4.8) and Eq. (4.15),

$$\frac{E}{N}(\rho, T = 0) = \frac{3}{5} \varepsilon_f + \frac{3}{80} (3t_1 + 5t_2) \rho k_f^2 + \frac{3}{8} t_o \rho + \frac{1}{16} t_3 \rho^{\sigma+1}. \quad (4.16)$$

One can calculate the binding energy and the saturation density by employing,

$$\left(\frac{\partial E}{\partial \rho} \right)_{\rho=\rho_o} = 0. \quad (4.17)$$

Now we move to the calculations for the finite system. In this case, we have to include the finite size effect parameter in our calculations. The density relation Eq.(4.6) for the NM needs to be modified for the finite system as

$$\rho = \frac{k_f^3}{6\pi^2} + a_F \left[- \left(\frac{4\pi\rho}{3A} \right)^{\frac{1}{3}} \frac{3k_f^2}{16\pi} + \left(\frac{4\pi\rho}{3A} \right)^{\frac{2}{3}} \frac{3k_f}{16\pi} \right]. \quad (4.18)$$

k_f is obtained from Eq.(4.18) numerically. Then we can use Eq.(4.16) with the help of Eq.(4.18) to calculate the binding energy for several symmetric nuclei. Finally, we can determine the value for a_F via fitting experimental data.

³It should be noted that we have to remove the rearrangement contribution.

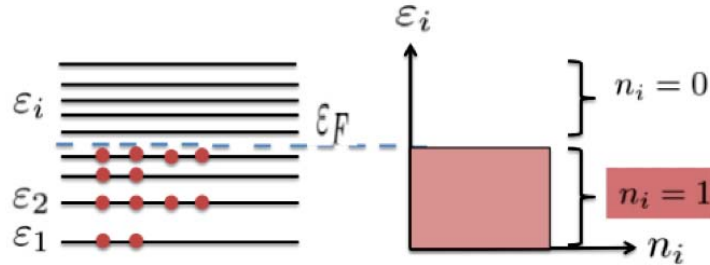


Figure 6: The indication of the fermi level distribution, where the energy, ε_i , and the occupation number, n_i , for the single particles are lower than the fermi energy, ε_f (Lacroix, 2011, P.10).

4.3 Liquid-Gas Phase Transition

It is well-known that a phase transition can only be observed in the thermodynamic limit (i.e. infinite system and constant density) where the phase transition can be seen as singularity behaviour (i.e. at least a sudden change). Such singularity will not appear in finite systems due to the partition function⁴ being an analytic function of the temperature and the full Hamiltonian [20, 53].

It is useful to clarify this point by considering the specific heat. The liquid-gas phase transition can be observed in infinite NM as the specific heat shows a sharp lambda-type singularity at the critical temperature $T_c(N)$. In a finite system, however, such a sharp singularity cannot appear for the specific heat, but it can be seen as a large peak at a limited temperature $T_{lim}(N)$ which trends to the critical temperature $T_c(N)$ when the

⁴The partition function is formed to present a statistical ensemble in order to extract thermodynamic variables of an equilibrium system [52].

number of particles approaches infinity [20]. Namely, the limited temperature $T_{lim}(N)$ that approaches $T_c(N)$ as $N \rightarrow \infty$ can be considered as $T_c(N)$ for the finite system. The critical temperature is shifted to a lower value and the singularity behaviour appears as finite peaks, resulting from the finite size effect [20].

4.4 Critical Temperature

The critical temperature can be generally determined from the inflection point of the pressure-density curves or the chemical potential-density curves,

$$\begin{aligned}\frac{\partial P}{\partial \rho} = 0 &= \frac{\partial^2 P}{\partial^2 \rho}, \\ \frac{\partial \mu}{\partial \rho} = 0 &= \frac{\partial^2 \mu}{\partial^2 \rho}.\end{aligned}\tag{4.19}$$

The two isotherms P vs ρ and μ vs ρ , are related via Helmholtz function,

$$P = \rho\mu - F,\tag{4.20}$$

where $F = \frac{E}{V}$ corresponds to Helmholtz function of free energy density, and

$$\mu = \left[\frac{\partial F}{\partial \rho} \right]_T.$$

From the above discussions, it seems that the EOS derived from P vs ρ isotherms is equivalent to that given by the μ vs ρ isotherms. Thus, rather than working with pressure, it is desirable to deal with the chemical potential for the following reason. In any system, there are different phases transitions, the pressure measuring is not simple due to the fact that the geometry of the boundary region can influence the determining of the pressure.

4.5 Chemical Potential

In this section we shall calculate the chemical potential for symmetric infinite NM and also a system consisting of N-nucleons in the framework of Hartree Fock. The method used here to find the chemical potential is given in Ref.[42].

The distribution of the momentum states, $n(k)$, follows the Fermi-Dirac distribution

$$n(k) = [1 + \exp(ke + u(k) + \mu)\beta]^{-1}, \quad (4.21)$$

where $ke = \frac{\hbar^2 k^2}{2m}$ is the kinetic energy of the single particle, $u(k)$ corresponds to the HF mean field, μ is the chemical potential, and $\beta = \frac{1}{k_B T}$.

As we can see the momentum distribution depends on the mean field as well as the chemical potential. The mean field has been previously found in Eq.(4.15), while the chemical potential can be readily obtained from inverting the total density relation. It is worth rewriting this relation Eq.(4.6),

$$\rho = v \int \frac{d^3 k}{(2\pi)^3} n(k). \quad (4.22)$$

At fixed temperature, we can self-consistently solve Eq.(4.21) and Eq.(4.22) by using a numerical method. Therefore, the chemical potential, μ , can be obtained as a function of the density, ρ . These processes are repeated many times for different temperatures until the critical temperature is found.

5 Results and Discussion

In this chapter, we present our results on determining the finite size effect parameter a_F and on the study of liquid-gas phase transition for nuclear matter and nuclei.

5.1 Zero Temperature Properties

In the zero temperature limit, the internal energy of the nuclear matter and nuclei becomes the ground state energies. The binding energy and the saturation density can be calculated by employing $(\frac{\partial E}{\partial \rho})_{\rho=\rho_o} = 0$, where

$$\frac{E}{N}(\rho, T = 0) = \frac{3}{5}\varepsilon_f + \frac{3}{80}(3t_1 + 5t_2)\rho k_f^2 + \frac{3}{8}t_o\rho + \frac{1}{16}t_3\rho^{\sigma+1}, \quad (5.1)$$

for the NM. The binding energy is given by $E(\rho = \rho_o, T = 0)$.

5.1.1 Infinite Nuclear Matter

In the case of infinity NM, it is found that the energy per nucleon determined by using the various versions of Skyrme interaction are between 15 and 16 MeV, while the saturation density is between 0.14 and 0.15 fm^{-3} . Table 4 displays our findings for the saturation properties given by using Skyrme interaction. These results are in good agreement with the experimental values $E_b \simeq 16$ MeV and $\rho_o \simeq 0.16 fm^{-3}$ [28]. The $E \sim \rho$ isotherms given by the five sets of Skyrme interaction are shown in Fig.7. It can be seen that all the five sets of Skyrme interaction follow a similar behaviour starting from the initial point until the saturation point, and then their behaviour slightly diverges.

Table 4: The saturation properties of nuclear matter calculated with different versions of Skyrme interaction.

Force	$E_b(\text{MeV})$	$\rho_o(\text{fm}^{-3})$
SKI	16.0	0.150
SKII	15.9	0.140
SKIII	15.8	0.140
SKIV	15.9	0.150
SKV	16.0	0.155

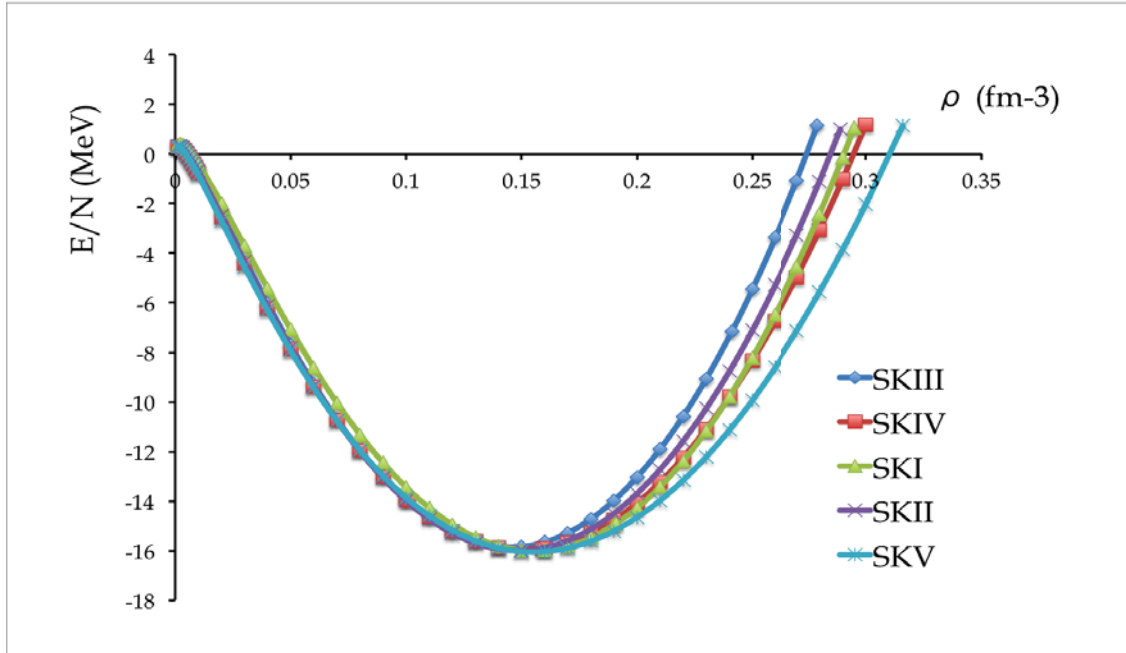


Figure 7: Nuclear matter $E \sim \rho$ isotherms calculated with SKI, SKII, SKIII, SKIV, and SKV interaction.

5.1.2 Finite Size Effect Parameter and Saturation Properties

The binding energies of five nuclei have been calculated in order to obtain the value of the finite size effect parameter a_F , which is introduced into the Hill-Wheeler formula,

$$dN_k = V \frac{k^2 dk}{2\pi^2} + a_F \left[- \left(\frac{4\pi\rho}{3A} \right)^{\frac{1}{3}} \frac{3kdk}{8\pi} + \left(\frac{4\pi\rho}{3A} \right)^{\frac{2}{3}} \frac{3dk}{16\pi} \right]. \quad (5.2)$$

The parameter a_F is determined by fitting the calculated binding energies with the experimental data⁵.

The obtained values for a_F for different sets of Skyrme force are given in Table 5, while the zero temperature properties calculated with Eq.(5.2) for several nuclei are listed in Table 6. We found that the binding energies of the five nuclei are generally in good agreement with the experimental data. However, for the SKI force one needs a very small value of a_F in order to achieve a better agreement between theoretical calculation and experimental data. This may indicate some problems in the calculations or in the force itself.

The saturation densities ρ_o of these nuclei given by the various sets of Skyrme interaction are between 0.13 and 0.22 fm^{-3} . Only the densities given by SKI and SKIII interaction are in good agreement with $\rho_o = 0.13fm^{-3}$ that is obtained in Ref.[2] by employing the phenomenological formula $R = r_o A^{\frac{1}{3}}$ and $R = (3/4\pi\rho_o)^{\frac{1}{3}}$, with $r_o = 1.21 \sim 1.22$.

Fig. 8 shows the $E \sim \rho$ isotherms for ${}^{56}_{28}Ni$ calculated by employing SKIV interaction and Eq.(5.2) for $a_F = 1.0$ and 0.55. The calculation with $a_F = 1.0$ does not allow the formation of a bound state. This suggests that it is necessary to study the finite size effect of a nucleus with the modified Hill-Wheeler formula with $a_F \neq 1.0$.

⁵The experimental data is taken from Ref. [54].

It is found that each set of Skyrme interaction takes a different value of a_F apart from SKI and SKIII forces which lead to the same value of $a_F = 0.01$. This difference in the value of a_F for different versions of Skyrme force is expected. As we noticed from previous studies the properties of NM employing several sets of Skyrme interaction were distinguishable from each other. For example, the critical points as well as the effective masses at the critical density and the saturation density employing several sets of Skyrme interaction are different as found in Ref. [24]. Table 7 indicates the different values of the NM properties obtained in Ref. [24]. Also, they found from an extensive detailed comparison that the behaviour of each version of Skyrme force is different from the other.

In our opinion, this difference in a_F values might result from the difference in values of the forces parameters (t_o, t_1, t_2, t_3) , especially, t_2 . As it is obvious from our results, this parameter may be the main reason for resulting different values of a_F . The smallest value of $a_F = 0.01$ is given by SKI and SKIII which take the smallest values of t_2 , while the largest value of $a_F = 0.55$ is given by the SKV interaction which takes the largest value of t_2 .

Also, we found that the only SKV interaction gives a value of a_F that is consistent with that given in Ref.[2] by employing Gogny D1 effective interaction.

Table 5: The calculated values of a_F with different versions of Skyrme interaction.

Force	SKI	SKII	SKIII	SKIV	SKV
a_F	0.01	0.17	0.01	0.35	0.55

Table 6: The saturation properties for different nuclei obtained with different versions of Skyrme interaction, where (Exp.) means the experimental data.

Nuclei		${}^{80}_{40}\text{Zr}$	${}^{56}_{28}\text{Ni}$	${}^{40}_{20}\text{Ca}$	${}^{36}_{18}\text{Ar}$	${}^{28}_{14}\text{Si}$
Binding Energy(E_b) MeV	Exp.	8.37	8.64	8.55	8.51	8.44
	SKI	6.49	6.48	6.48	6.48	6.47
	SKII	7.34	7.89	8.25	8.34	7.40
	SKIII	8.44	8.47	8.49	8.50	8.51
	SKIV	8.56	8.61	8.45	8.37	7.60
	SKV	9.92	8.69	7.31	6.84	5.70
Saturation Density (ρ_o) fm^{-3}	SKI	0.13	0.13	0.13	0.13	0.13
	SKII	0.16	0.16	0.16	0.16	0.15
	SKIII	0.13	0.13	0.13	0.13	0.13
	SKIV	0.19	0.18	0.18	0.18	0.18
	SKV	0.24	0.22	0.21	0.21	0.20

Table 7: The values of some properties for nuclear matter obtained in Ref.[24] employing several sets of Skyrme interaction, where the effective masses at the critical density and at the saturation density are denoted by $(m^*/m)_c$ and $(m^*/m)_o$, respectively.

Properties	SKI	SKII	SKIII	SKIV	SKV
$T_c(MeV)$	20.12	16.75	17.95	16.00	14.55
$\rho_c(fm^{-3})$	0.061	0.580	0.056	0.057	0.048
$(m^*/m)_c$	0.963	0.779	0.893	0.703	0.744
$(m^*/m)_o$	0.913	0.577	0.760	0.471	0.382

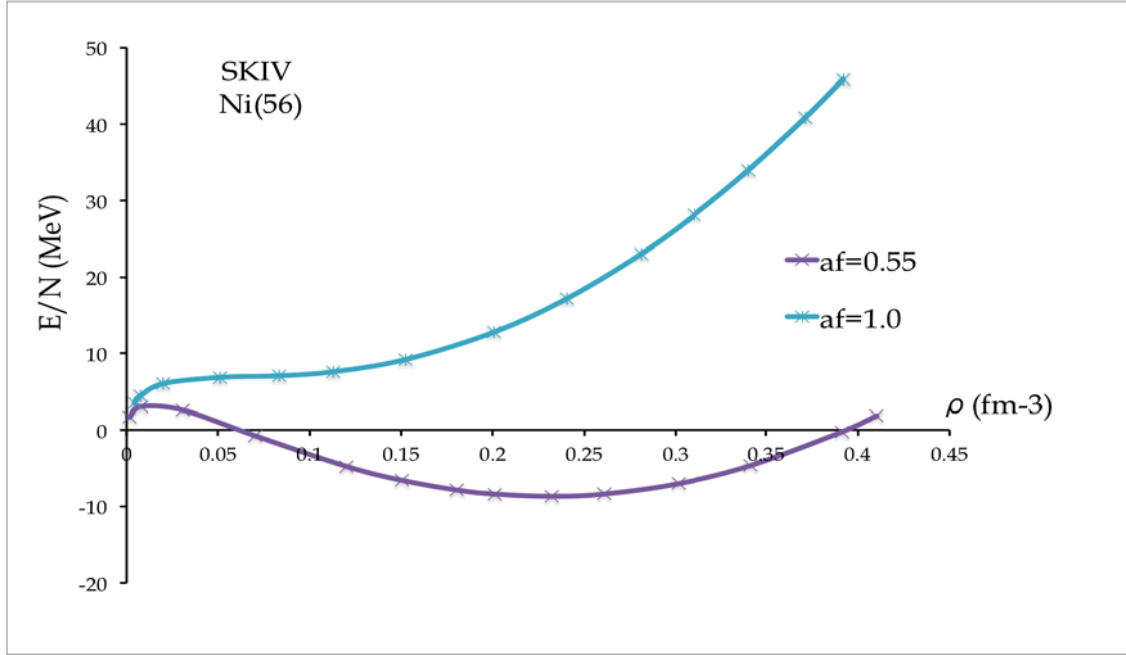


Figure 8: The $E \sim \rho$ isotherms for ${}^{56}_{28}\text{Ni}$ obtained from Eq.(5.2) with $a_F = 1.0$ and 0.55 given by SKIV interaction.

5.2 Liquid-Gas Phase Transition

We have solved self-consistently the equation of state at finite temperature that was introduced in Chapter 4. The chemical potential and the density are extracted at each point in the iterative procedure. Thus, the chemical potential is plotted as a function of density and the $\mu \sim \rho$ isotherms have been used to determine the critical temperature and the critical density. In what follows the critical temperature (T_c) and the critical density (ρ_c) have been extracted for the NM and finite size systems.

5.2.1 Infinite Nuclear Matter

The $\mu \sim \rho$ isotherms for the nuclear matter calculated with the SKI interaction at different temperatures are shown in Fig.9.

The critical temperature and density calculated are listed in Table 8. It is found that the critical points of infinite NM obtained by the different sets of Skyrme interaction are not identical. The $\mu \sim \rho$ isotherms for the NM calculated with different sets of Skyrme interaction at $T=16$ MeV are shown in Fig.10. The isotherms calculated with the SKI and SKIII are similar, while the other isotherms are distinguishable from each other.

The critical temperatures are found to be in the range of 21.69 MeV \sim 39.45 MeV, while the critical densities are between 0.06 and 0.14 fm^{-3} . Our findings disagree with that given in Ref. [24] apart from SKI interaction. The results given in Ref.[24] are included in Table 8. This unambiguous difference between the results found here and that found in Ref.[24] might come from using different methods for the calculations. A real time Green's function method is used in Ref.[24]. In the next part we will discuss the finite size case.

Table 8: The critical values of the temperature $T_c(MeV)$ and the density $\rho_c(fm^{-3})$ calculated in this work and in Ref.[24] for an infinite nuclear matter with different versions of Skyrme interaction.

	Critical Points	SKI	SKII	SKIII	SKIV	SKV
This work	$T_c(MeV)$	21.687	24.090	21.650	28.340	39.450
	$\rho_c(fm^{-3})$	0.064	0.075	0.062	0.095	0.146
Ref.[24]	$T_c(MeV)$	20.030	16.480	17.920	16.610	16.770
	$\rho_c(fm^{-3})$	0.05 \sim 0.06 fm^{-3}				

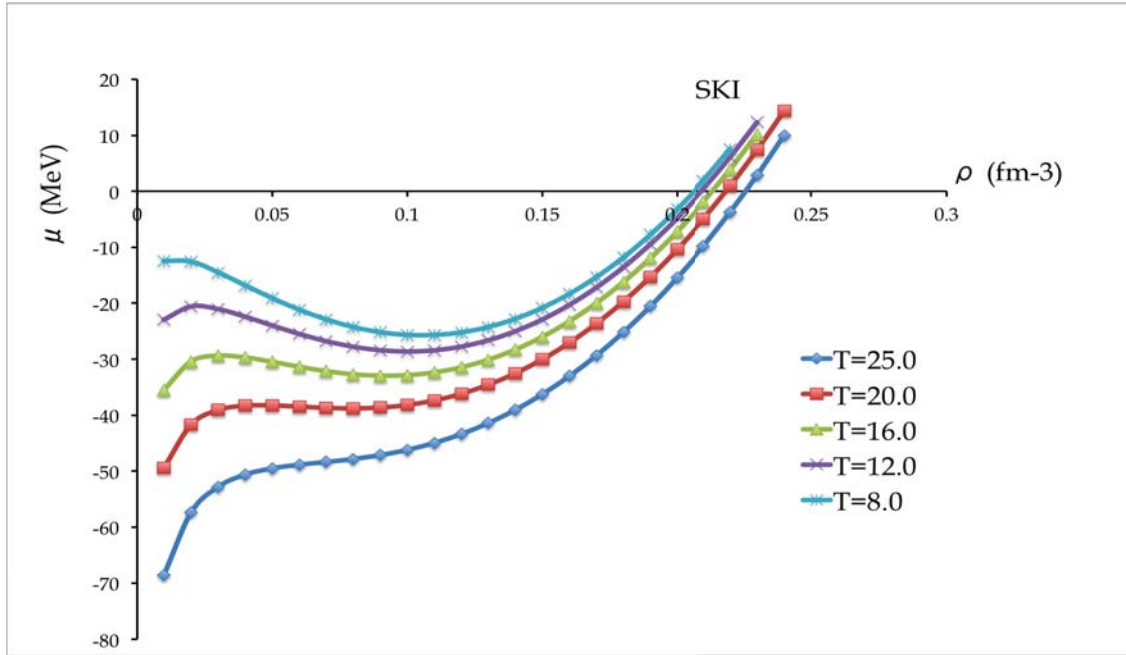


Figure 9: Nuclear matter $\mu \sim \rho$ isotherms calculated with SKI interaction at different temperatures.

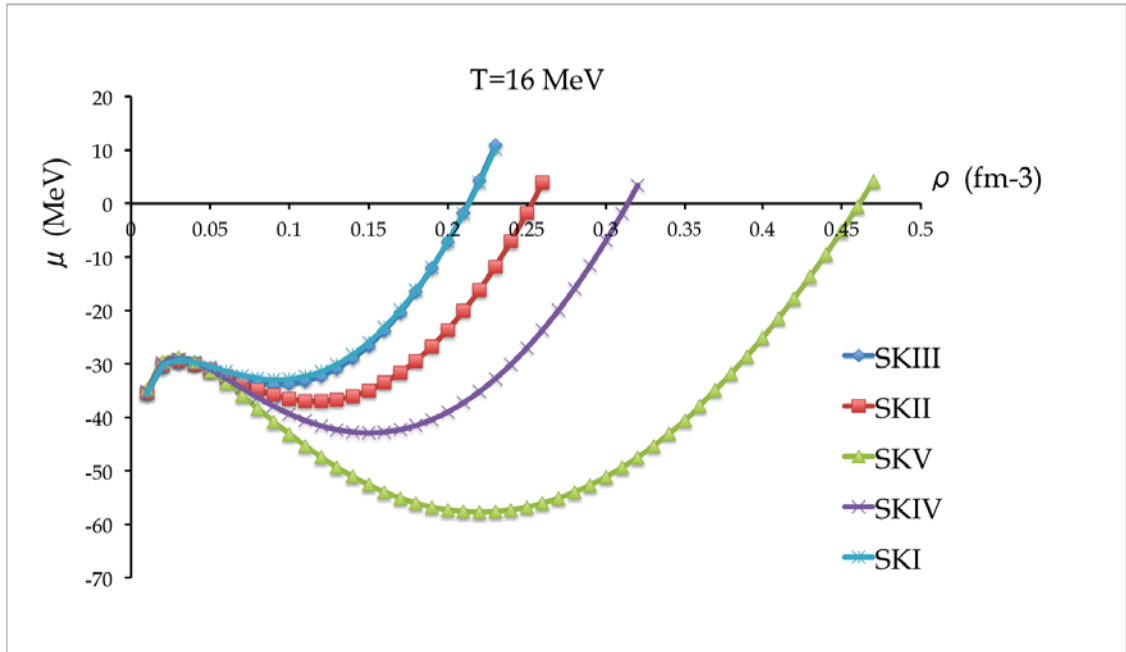


Figure 10: Nuclear matter $\mu \sim \rho$ isotherms calculated with SKI, SKII, SKIII, SKIV, and SKV interactions at $T=16$ MeV.

5.2.2 Finite Size Systems

We have determined the critical temperature and density for systems with a finite number of nucleons ($N=100,1000,10000$). The finite size effect has been taken into account by inserting the parameter of finite size effect a_F where it takes different values depending on the set of Skyrme interaction employed.

The $\mu \sim \rho$ isotherms have been calculated for a different number of nucleons N at finite temperature. Fig.11 shows the $\mu \sim \rho$ isotherms for SKIV interaction with different N at $T=16.0$ MeV. As it can be seen, the chemical potential decreases as N increase. This means the size of the nucleons has a significant effect on the findings for the different sets of Skyrme interaction. Furthermore, we have found various isotherms for SKII interaction at various temperatures where the number of nucleons is fixed, as plotted in Fig.12. One can see that increasing the temperature leads to a decrease in the chemical potential.

The critical features obtained for the different sizes using the various sets of Skyrme interaction are listed in Table 9. It is found that the critical values given by different versions of Skyrme interaction are different from each other, apart from SKI and SKIII interactions.

It is found that the critical temperature calculated with the SKV interaction drops by about 8 MeV when N is changed from 10000 to 100, while the T_c calculated with the other versions of Skyrme interaction only drops by about $1 \sim 3$ MeV.

We found that the critical features obtained from our calculations with Eq.(5.2) by inserting the value of a_F are very different from that with Eq.(4.4) for all Skyrme interaction, except for SKI. The critical points determined with Eq.(4.4) and reported in Ref.[15] are listed in Table 10. The critical temperatures calculated in this work are much larger than those found in Ref.[15]. For example, the T_c calculated in our work with SKV interaction for $N=10000$ is 36.43 MeV which is larger by about 24.17 MeV than that found in Ref.[15]. Additionally, we noticed in our findings that the difference between the critical temperatures for the different N employing the different sets of Skyrme force, except SKV is small. Such a small difference was not reported in Ref. [15].

From Table 9, one can conclude that the finite size effect parameter a_F plays a role in reducing the difference in the calculation for the critical temperature for the finite nuclei employing various sets of the Skyrme force.

Figs. 13 and 14 illustrate the difference between the isotherms calculated with Eq.(5.2) and with Eq.(4.4).

Table 9: The critical values of the temperature $T_c(MeV)$ and the density $\rho_c(fm^{-3})$ for different sizes calculated with different versions of Skyrme interaction.

Number of Nucleons	Critical Points	SKI	SKII	SKIII	SKIV	SKV
10000	$T_c(MeV)$	21.68	23.84	21.64	27.51	36.43
	$\rho_c(fm^{-3})$	0.062	0.074	0.062	0.094	0.135
1000	$T_c(MeV)$	21.67	23.57	21.63	26.59	33.30
	$\rho_c(fm^{-3})$	0.063	0.073	0.061	0.091	0.122
100	$T_c(MeV)$	21.66	23.05	21.60	24.85	27.70
	$\rho_c(fm^{-3})$	0.062	0.073	0.061	0.084	0.104

Table 10: The values of the critical points for different sizes (N=100, 1000, 10000) obtained in a previous study [15] with Eq.(4.4) using Skyrme interaction.

Critical Temperature $T_c(MeV)$					
Number of Nucleons	SKI	SKII	SKIII	SKIV	SKV
10000	19.06	15.12	16.48	14.66	12.26
1000	17.96	13.34	15.53	12.43	11.56
100	15.25	9.71	12.69	8.31	6.56
Critical Density(ρ_c)=0.05 ~ 0.06 fm^{-3}					

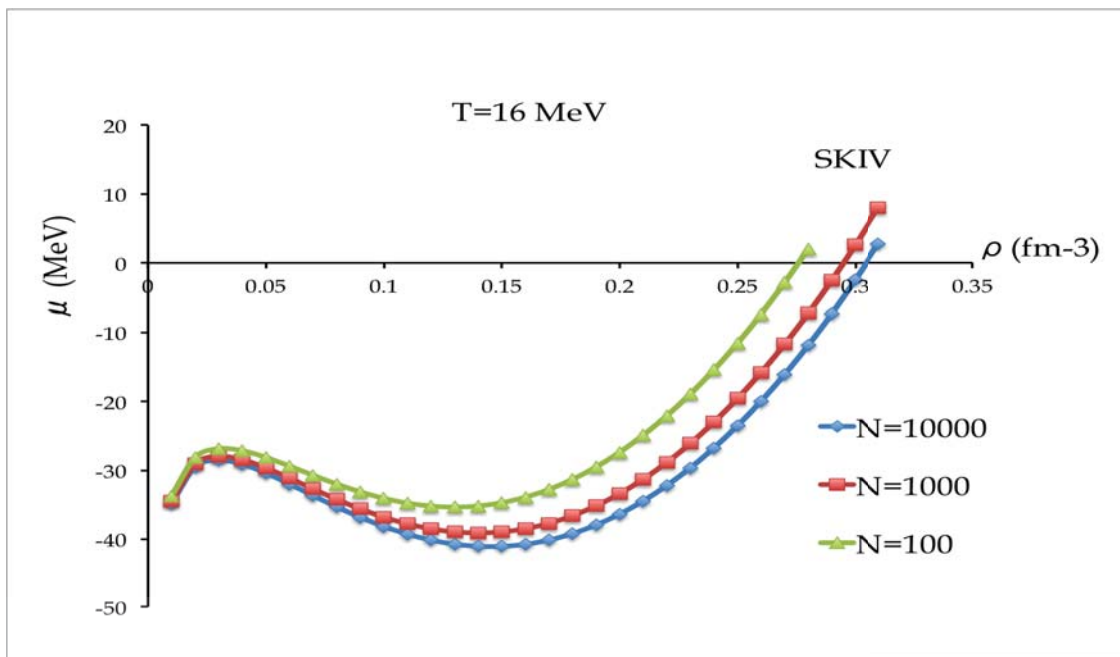


Figure 11: The $\mu \sim \rho$ isotherms calculated with SKIV interaction in different sizes at $T=16.0$ MeV.

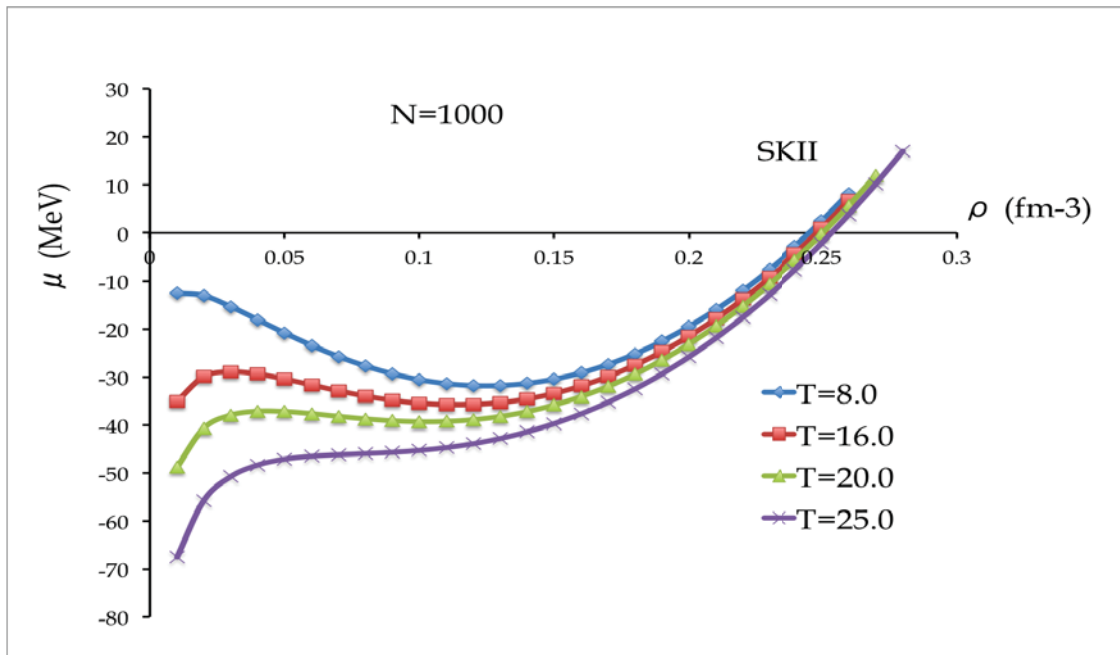


Figure 12: The $\mu \sim \rho$ isotherms calculated for $N=1000$ with SKII interaction at different temperatures.

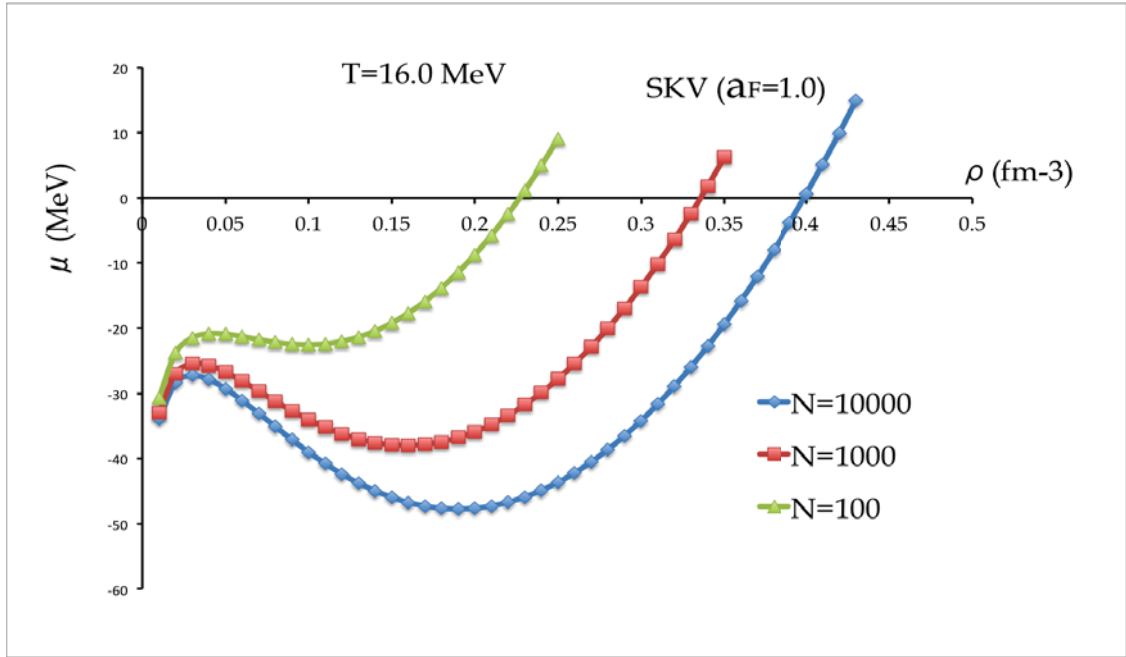


Figure 13: The $\mu \sim \rho$ isotherms calculated with Eq.(4.4) and SKV interaction in different sizes at $T=16.0$ MeV.

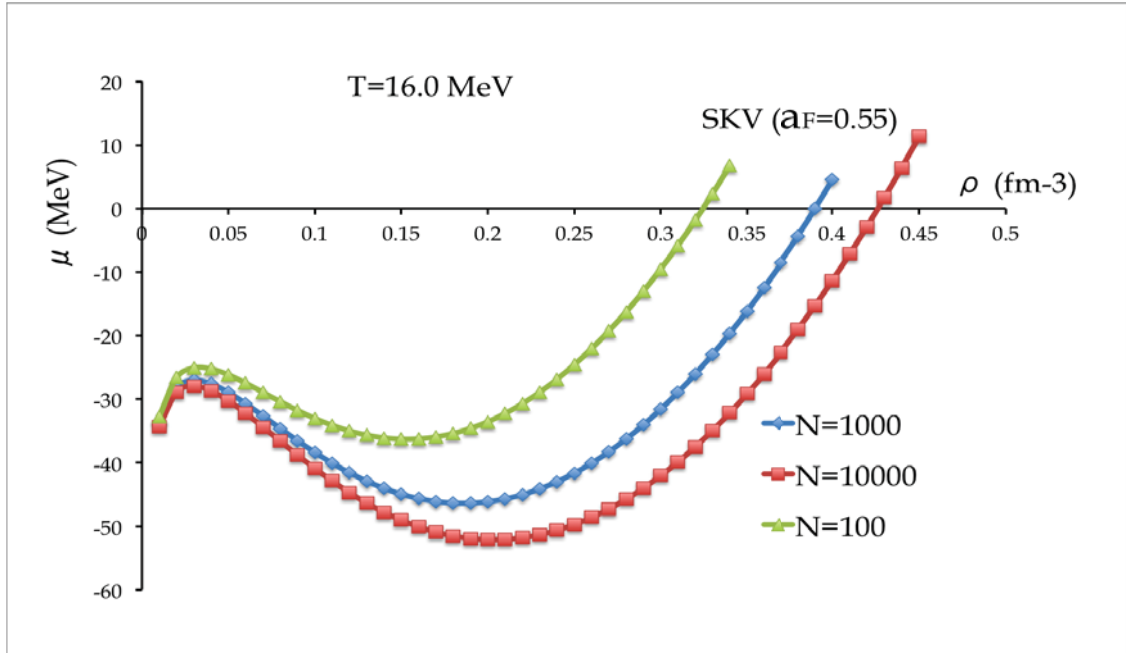


Figure 14: The $\mu \sim \rho$ isotherms calculated with Eq.(5.2) and SKV interaction in different sizes at $T=16.0$ MeV.

6 Summary and Conclusion

The equation of state for nuclear matter and finite nuclei has been studied using self-consistent Hartree Fock approximation and mean field theory. The Skyrme effective nuclear force and the Hill-Wheeler formula are employed in the calculation. The finite size effect parameter a_F is determined by comparing theoretical calculations and experimental results for the saturation properties.

The effective interaction employed has a great influence on the value of a_F ; different versions of Skyrme force lead to different values for a_F apart from SKI and SKIII which give a similar value for a_F . Also, a_F values obtained with Skyrme interaction are generally different from that obtained with Gogny force with the exception of SKV interaction which gives a similar value for a_F as the D1 Gogny interaction.

The zero temperature properties of the nuclear matter calculated with the Skyrme interaction are consistent with the experimental data. In the case of finite nuclei, we found a value of $a_F < 1$ is essential for the formation of a bound state of nucleons. The calculated zero temperature properties for the finite nuclei are reasonable, but the saturation densities given by SKV interaction are larger than $\rho_o = 0.13 fm^{-3}$ which is obtained by using a phenomenological formula.

The critical points of the first order phase transition for the nuclear matter and finite size nuclei calculated with the several versions of Skyrme force are distinguishable from each other. The largest value of critical temperature for nuclear matter is given by SKV force as $T_c = 39.45 MeV$, while SKIII interaction gives the smallest value as $T_c = 21.65 MeV$. Similarly, the largest value of the critical density is given by SKV interaction as $\rho_c = 0.146 fm^{-3}$. It is found that the critical temperature decreases as the number of nucleons in the system decreases.

The critical features calculated with a_F are significantly different from those calculated with $a_F = 1.0$. We can conclude that the inclusion of the finite size parameter a_F leads to a reduction in the difference between the chemical potential \sim density isotherms obtained for systems with different numbers of nucleons.

Our results for the liquid-gas phase transition are different from that presented in a previous study, which requires further investigation. In the future study, it is of interest to calculate the pressure \sim density isotherms and make a comparison with the results reported in this work.

References

- [1] Y. Luo, G. Jin, J. Liu, *Heavy Ion Physics and Its Applications*, World Scientific, **1996**.
- [2] F.-G. Cao, S.-D. Yang, *arXiv preprint nucl-th/9612022* **1996**.
- [3] E. Suraud, C. Gregoire, B. Tamain, *Progress in particle and nuclear physics* **1989**, *23*, 357–467.
- [4] Y.-J. Zhang, R.-K. Su, H. Song, F.-M. Lin, *Physical Review C* **1996**, *54*, 1137.
- [5] A. Panagiotou, M. Curtin, H. Toki, D. Scott, P. Siemens, *Physical Review Letters* **1984**, *52*, 496.
- [6] Z. Chen, C. Gelbke, W. Gong, Y. Kim, W. Lynch, M. Maier, J. Pochodzalla, M. Tsang, F. Saint-Laurent, D. Ardouin, et al., *Physical Review C* **1987**, *36*, 2297.
- [7] G. Sauer, H. Chandra, U. Mosel, *Nuclear Physics A* **1976**, *264*, 221–243.
- [8] D. Brink, E. Boeker, *Nuclear Physics A* **1967**, *91*, 1–26.
- [9] H. Song, R. Su, *Physical Review C* **1991**, *44*, 2505.
- [10] H. Song, Z. Qian, R. Su, *Physical Review C* **1993**, *47*, 2001.
- [11] H. Song, Z. Qian, R. Su, *Physical Review C* **1994**, *49*, 2924.
- [12] M. Abd-Alla, S. Ramadan, M. Hassan, *Physical Review C* **1987**, *36*, 1565.
- [13] L. Satpathy, M. Mishra, R. Nayak, *Physical Review C* **1989**, *39*, 162.
- [14] J. Treiner, H. Krivine, *Journal of Physics G: Nuclear Physics* **1976**, *2*, 285.
- [15] R.-K. Su, F.-M. Lin, *Physical Review C* **1989**, *39*, 2438.
- [16] H.-Q. Song, G.-D. Zheng, R.-K. Su, *Journal of Physics G: Nuclear and Particle Physics* **1990**, *16*, 1861.
- [17] M. Baldo, L. Ferreira, *Physical Review C* **1999**, *59*, 682.
- [18] H. Jaqaman, A. Mekjian, L. Zamick, *Physical Review C* **1983**, *27*, 2782.
- [19] H. H. Gutbrod, A. Warwick, H. Wieman, *Nuclear Physics A* **1982**, *387*, 177–189.
- [20] H. Jaqaman, A. Mekjian, L. Zamick, *Physical Review C* **1984**, *29*, 2067.

- [21] J. W. Negele, *Physical review C* **1970**, *1*, 1260.
- [22] R.-K. Su, F.-M. Lin, *Journal of Physics G: Nuclear and Particle Physics* **1989**, *15*, 1591.
- [23] N.-P. WANG, S.-D. YANG, **1992**.
- [24] R. Su, S. Yang, T. Kuo, *Physical Review C* **1987**, *35*, 1539.
- [25] A. R. Huguet, PhD thesis, PhD thesis. Universitat de Barcelona, 2007. url: <http://personal.ph.surrey.ac.uk/~m01088/files/thesis.pdf> (cit. on p. 32), **2007**.
- [26] I. Białyński-Birula, M. Cieplak, J. Kamiński, *Theory of quanta*, Oxford University Press Oxford, **1992**.
- [27] A. L. Fetter, J. D. Walecka, *Quantum theory of many-particle systems*, Courier Corporation, **2012**.
- [28] D. Lacroix in Ecole Joliot-Curie” Physics at the femtometer scale”, **2011**.
- [29] P. Ring, P. Schuck, *The nuclear many-body problem*, Springer Science & Business Media, **2004**.
- [30] K. Moghrabi, PhD thesis, Institut de Physique Nucléaire d’orsay, Université paris-sud XI, **2013**.
- [31] P. Bonche, D. DPhG, Thermodynamical description of excited nuclei, tech. rep., CEA Centre d’Etudes Nucleaires de Saclay, **1989**.
- [32] B. Povh, K. Rith, F. Zetsche, *Particles and nuclei, Vol. 1*, Springer, **1995**.
- [33] P. Hohenberg, W. Kohn, *Physical review* **1964**, *136*, B864.
- [34] J. R. Stone, P.-G. Reinhard, *Progress in Particle and Nuclear Physics* **2007**, *58*, 587–657.
- [35] E. Lipparini, *Modern many-particle physics: atomic gases, nanostructures and quantum liquids*, World Scientific Publishing Co Inc, **2008**.
- [36] J. C. Slater, *Physical Review* **1951**, *81*, 385.
- [37] P.-A. Martin, F. Rothen, *Many-body problems and quantum field theory: an introduction*, Springer Science & Business Media, **2013**.

-
- [38] K. Capelle, *arXiv preprint cond-mat/0211443* **2002**.
- [39] V. Soma, P. Bozek, *arXiv preprint nucl-th/0609044* **2006**.
- [40] D. Vautherin, D. t. Brink, *Physical Review C* **1972**, *5*, 626.
- [41] A. A. Alzubadi, Z. Dakhil, S. T. Aluboodi, *Journal of Nuclear and Particle Physics* **2014**, *4*, 155–163.
- [42] A. Rios, *Nuclear Physics A* **2010**, *845*, 58–87.
- [43] F. Chappert, M. Girod, S. Hilaire, *Physics Letters B* **2008**, *668*, 420–424.
- [44] J. Dechargé, D. Gogny, *Physical Review C* **1980**, *21*, 1568.
- [45] T. Skyrme, *Philosophical Magazine* **1956**, *1*, 1043–1054.
- [46] J. Friedrich, P.-G. Reinhard, *Physical Review C* **1986**, *33*, 335.
- [47] A. K. Vuong, PhD thesis, Texas A&M University, **2007**.
- [48] J. Bell, T. Skyrme, *Philosophical Magazine* **1956**, *1*, 1055–1068.
- [49] Y. Engel, D. Brink, K. Goeke, S. Krieger, D. Vautherin, *Nuclear Physics A* **1975**, *249*, 215–238.
- [50] J. R. Stone, J. Miller, R. Koncewicz, P. Stevenson, M. Strayer, *Physical Review C* **2003**, *68*, 034324.
- [51] D. X. Roca-Maza, G. Colo, G. Accorto, PhD thesis.
- [52] J. A. López, C. Dorso, *Lectures Notes On Phase Transformations In Nuclear Matter*, World Scientific, **2000**.
- [53] K. Binder, D. Landau, *Physical Review B* **1984**, *30*, 1477.
- [54] G. Audia, A. Wapstrab, C. Thibaulta, *Nuclear Physics A* **2003**, *729*, 337–676.

A Appendix

The identities used in the energy density calculations are included in this appendix. First, it is assumed that the single particle state $|i\rangle$ is invariant under time reversal. This means the state of the time reversal, $|\vec{i}\rangle = K|i\rangle$, is occupied as well. Therefore the operator of the time reversal can be formed as, $K = -i\hat{S}_y K^*$, where K^* corresponds to the operator of the complex-conjugation. The state of single particle under time reversal is given by

$$\varphi_i^-(r, s, \tau) = -i \sum_{s'} \langle s | \hat{S}_y | s' \rangle, \quad (\text{A.1})$$

where r , s and τ denote the coordinates of space, spin and isospin of the nucleon, respectively. The spin operator S_y can be described by the Pauli matrix ,

$$S_y = \begin{bmatrix} 0 & -i \\ i & 0 \end{bmatrix}, \quad (\text{A.2})$$

and the states for spin up, $S_{+\frac{1}{2}}$, and spin down, $S_{-\frac{1}{2}}$, are given by

$$S_{+\frac{1}{2}} = \begin{bmatrix} 1 \\ 0 \end{bmatrix}, \quad S_{-\frac{1}{2}} = \begin{bmatrix} 0 \\ 1 \end{bmatrix}. \quad (\text{A.3})$$

We also used

$$\langle s | \hat{S}_y | s' \rangle = -2is\delta_{-s, s'}. \quad (\text{A.4})$$

Thus

$$\varphi_i^-(r, s, \tau) = -2s\varphi_i^*(r, -s, \tau). \quad (\text{A.5})$$

It is assumed that the time-reversed states are invariant, thus we have

$$\begin{aligned}
 & \sum_i \varphi_i^*(r, s_1, \tau) \varphi_i(r, s_2, \tau) \\
 &= \frac{1}{2} \sum_i [\varphi_i^*(r, s_1, \tau) \varphi_i(r, s_2, \tau) + \varphi_i^{-*}(r, s_1, \tau) \varphi_i^-(r, s_2, \tau)] \\
 &= \frac{1}{2} \sum_i [\varphi_i^*(r, s_1, \tau) \varphi_i(r, s_2, \tau) + 4s_1 s_2 \varphi_i^*(r, -s_1, \tau) \varphi_i(r, -s_2, \tau)].
 \end{aligned} \tag{A.6}$$

Therefore, for the case $s_1 = s_2$, one has

$$\begin{aligned}
 \sum_i \varphi_i^*(r, s_1, \tau) \varphi_i(r, s_1, \tau) &= \frac{1}{2} \sum_i [\varphi_i^*(r, s_1, \tau) \varphi_i(r, s_1, \tau) + \varphi_i^*(r, -s_1, \tau) \varphi_i(r, -s_1, \tau)] \\
 &= \frac{1}{2} \sum_{is} [\varphi_i^*(r, s_1, \tau) \varphi_i(r, s_1, \tau)] = \frac{1}{2} \rho_\tau(r),
 \end{aligned} \tag{A.7}$$

and for the case $s_1 = -s_2$, one has

$$\sum_i \varphi_i^*(r, s_1, \tau) \varphi_i(r, -s_1, \tau) = 0. \tag{A.8}$$

Therefore, one obtains

$$\sum_i \varphi_i^*(r, s_1, \tau) \varphi_i(r, -s_2, \tau) = \frac{1}{2} \delta_{s_1 s_2} \rho_\tau(r). \tag{A.9}$$

Using identities

$$\begin{aligned}
 \langle s | S_x | s' \rangle &= \delta_{s, s'}, \\
 \langle s | S_y | s' \rangle &= -2is \delta_{s, s'}, \\
 \langle s | S_z | s' \rangle &= 2s \delta_{s, s'},
 \end{aligned} \tag{A.10}$$

one has

$$\sum_{is_1 s_2} \varphi_i^*(r, s_1, \tau) \langle s_1 | \vec{s} | s_2 \rangle \varphi_i(r, s_2, \tau) = 0. \tag{A.11}$$